

1 **Population Normalization in SARS-CoV-2 Wastewater-Based Epidemiology: Implications**  
2 **from Statewide Wastewater Monitoring in Missouri**

3  
4 Chenhui Li<sup>1</sup>, Mohamed Bayati<sup>1</sup>, Shu-Yu Hsu<sup>1,2</sup>, Hsin-Yeh Hsieh<sup>1</sup>, Wilfing Linds<sup>1</sup>, Anthony  
5 Belenchia<sup>3</sup>, Sally A. Zemmer<sup>4</sup>, Jessica Klutts<sup>4</sup>, Mary Samuelson<sup>4</sup>, Melissa Reynolds<sup>3</sup>, Elizabeth  
6 Semkiw<sup>3</sup>, Hwei-Yiing Johnson<sup>3</sup>, Trevor Foley<sup>5</sup>, Chris G. Wieberg<sup>4</sup>, Jeff Wenzel<sup>3</sup>, Terri D.  
7 Lyddon<sup>6</sup>, Mary LePique<sup>6</sup>, Clayton Rushford<sup>6</sup>, Braxton Salcedo<sup>6</sup>, Kara Young<sup>6</sup>, Madalyn  
8 Graham<sup>6</sup>, Reinier Suarez<sup>6</sup>, Anarose Ford<sup>6</sup>, Dagmara S. Antkiewicz<sup>7</sup>, Kayley H. Janssen<sup>7</sup>, Martin  
9 M. Shafer<sup>7</sup>, Marc C. Johnson<sup>6</sup>, Chung-Ho Lin<sup>1,2\*</sup>

10 \*Corresponding Author:

11 Email address: [linchu@missouri.edu](mailto:linchu@missouri.edu)

12

13 **AFFILIATIONS**

14 <sup>1</sup> School of Natural Resources, University of Missouri, Columbia, MO 65211, USA.

15 <sup>2</sup> Center for Agroforestry, University of Missouri, Columbia, MO 65211, USA.

16 <sup>3</sup> Bureau of Environmental Epidemiology, Division of Community and Public Health, Missouri  
17 Department of Health and Senior Services, Jefferson City, MO 65109, USA

18 <sup>4</sup> Water Protection Program, Missouri Department of Natural Resources, Jefferson City, MO  
19 65101, USA

20 <sup>5</sup> Missouri Department of Corrections, Jefferson City, MO 65109, USA

21 <sup>6</sup> Department of Molecular Microbiology and Immunology, University of Missouri, School of  
22 Medicine and the Christopher S. Bond Life Sciences Center, Columbia, MO 65211, USA.

23 <sup>7</sup> Wisconsin State Laboratory of Hygiene, University of Wisconsin Madison, Madison, WI  
24 53718, USA

25

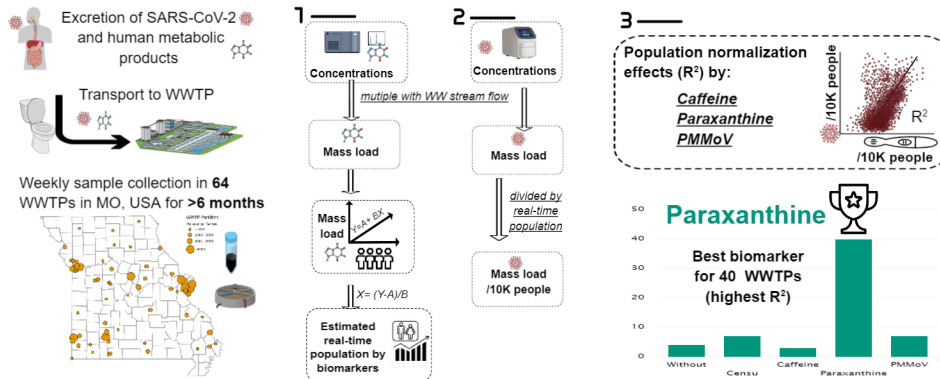
26

27

28 **KEYWORDS:** wastewater-based epidemiology; normalization biomarkers; real-time  
29 population; caffeine, paraxanthine, pepper mild mottle virus; wastewater SARS-CoV-2  
30 concentration; COVID-19 incidence rate

31

## 32 ABSTRACT



33

34 The primary objective of this study was to identify a universal wastewater biomarker for  
35 population normalization for SARS-CoV-2 wastewater-based epidemiology (WBE). A total of  
36 2,624 wastewater samples (41 weeks) were collected weekly during May 2021- April 2022 from  
37 64 wastewater facilities across Missouri, U.S. Three wastewater biomarkers, caffeine and its  
38 metabolite, paraxanthine, and pepper mild mottle virus (PMMoV), were compared for the  
39 population normalization effectiveness for wastewater SARS-CoV-2 surveillance. Paraxanthine  
40 had the lowest temporal variation and strongest relationship between population compared to  
41 caffeine and PMMoV. This result was confirmed by data from ten different Wisconsin's  
42 WWTPs with gradients in population sizes, indicating paraxanthine is a promising biomarker of  
43 the real-time population across a large geographical region. The estimated real-time population  
44 was directly compared against the population patterns with human movement mobility data. Of  
45 the three biomarkers, population normalization by paraxanthine significantly strengthened the  
46 relationship between wastewater SARS-CoV-2 viral load and COVID-19 incidence rate the most  
47 (40 out of 61 sewersheds). Caffeine could be a promising population biomarker for regions  
48 where no significant exogenous caffeine sources (e.g., discharges from food industries) exist. In  
49 contrast, PMMoV showed the highest variability over time, and therefore reduced the strength of  
50 the relationship between sewage SARS-CoV-2 viral load and the COVID-19 incidence rate, as  
51 compared to wastewater data without population normalization and the population normalized by  
52 either recent Census population or the population estimated based on the number of residential  
53 connections and average household size for that municipality from the Census. Overall, the  
54 findings of this long-term surveillance study concluded that the paraxanthine has the best  
55 performance as a biomarker for population normalization for SARS-CoV-2 wastewater-based  
56 epidemiology.

## 57 1. INTRODUCTION

58 Wastewater-based epidemiology (WBE) provides human activity information within  
59 sewershed boundaries by relating concentrations of chemical and biological “waste” materials in

60 wastewater influent to population-scale use, consumption of pharmaceuticals, illicit drugs, or  
61 rates of exposure to industrial chemicals.<sup>1</sup> Over the last few years, WBE applications have been  
62 emerging in infectious diseases or pathogens and antibiotic resistance, especially since the  
63 COVID-19 pandemic. The WBE is widely recognized as a valuable tool for monitoring  
64 community trends in COVID-19 with the advantages of providing an efficient and representative  
65 population-pooled sample, and complementing community data, especially where timely  
66 COVID-19 clinical testing is underused or unavailable.<sup>2</sup> Moreover, WBE reveals the  
67 underestimation of COVID-19 clinical testing because SARS-CoV-2 is shed by people with and  
68 without symptoms.<sup>3,4</sup> The WBE can also provide a useful early warning of the emergence or re-  
69 emergence of COVID-19 in a community, and afford timely insights for public health  
70 interventions, with previous studies showing that SARS-CoV-2 could be detected in wastewater  
71 up to two weeks before the cases were reported.<sup>5</sup> Furthermore, wastewater surveillance can be  
72 implemented in most communities since municipal wastewater collection systems serve nearly  
73 80 percent of U.S. households.<sup>6</sup>

74 The utility of WBE for cost-effective surveillance of SARS-CoV-2 levels in communities  
75 was recognized early in the COVID-19 pandemic. However, substantive uncertainty remains in  
76 how best to account for the contributing population and fecal strength. Robust population  
77 biomarkers are necessary to determine the SARS-CoV-2 load per capita, such that 1) the changes  
78 in wastewater virus concentration due to the dilution (e.g., increased volume resulting from  
79 major rainfall events or receiving additional discharge from industrial or natural resources) and  
80 2) population dynamics, are accounted for. Wastewater viral loads change with the variations in  
81 daily wastewater flow, the proportion of industrial discharge, and the gross proportions of  
82 solids, which can be influenced by the design and condition of the wastewater collection system.<sup>7</sup>  
83 For example, SARS-CoV-2 concentration is influenced if the WWTP is receiving wastewater  
84 from a combined sewer system that collects domestic wastewater and rainwater runoff in the  
85 same pipe; the weather effects, such as precipitation and infiltration/inflow into the sewers,  
86 impact the human fecal concentration. In addition, the population size contributing to the  
87 sewershed is expected to change over the surveillance period (due to deaths, births, tourism,  
88 weekday commuters, pandemic lockdown, temporary workers, etc.).<sup>1</sup> Therefore, temporal  
89 variation in wastewater volume/strength and population size must be better accounted for to  
90 make results more comparable over time.<sup>8</sup> However, population normalization approaches are  
91 still under development, and few studies have compared approaches/biomarkers systematically  
92 for optimization of wastewater SARS-CoV-2 data for predicting the clinical prevalence of  
93 COVID-19.<sup>9</sup>

94 The population variation is usually monitored and normalized using human fecal or urine  
95 biomarkers. Suitable human population normalization controls should meet certain criteria.<sup>8,10,11</sup>  
96 For example, the chemical biomarkers should be specific to human metabolism, excreted into  
97 sewage, exogenous sources are minimal, minimal intra- and inter-individual variance in daily  
98 excretion, and levels in raw sewage well above the method detection limit. Furthermore, the  
99 biomarkers must be stable in the wastewater for a reasonable long time (e.g., during the transport  
100 from the toilet to the sampling point and during sampling, storage, and analysis).<sup>12</sup> In addition,  
101 there should be low variance in the per capita daily excretion and not be affected by  
102 environmental variables such as season, weather, or geographic location.<sup>8</sup>

103 Some commonly measured wastewater properties/chemicals, such as chemical and biological  
104 oxygen demand, and total nitrogen and phosphorus, have been explored for wastewater  
105 population indicators.<sup>13,14</sup> The disadvantage of these environmental parameters is that they are  
106 highly influenced by wastewater composition (i.e., industrial, domestic, or mixed) since they are  
107 not only shed by humans but also from exogenous sources such as food waste processed by  
108 garbage disposals and fertilizer runoff.<sup>8</sup> Ammonium originates from the breakdown of urea<sup>15</sup>  
109 and is introduced via toilets and routinely measured by WWTP as a water quality parameter,  
110 which is supposed to be less affected by non-human sources than chemical or biological oxygen  
111 demand and total phosphorous.<sup>16</sup> However, Sweetapple et al. found that population  
112 normalization by orthophosphate and ammonium did not result in improvement of correlations  
113 between wastewater SARS-CoV-2 data and indicators of COVID-19 prevalence.<sup>14</sup>

114 In addition, a variety of endogenous and exogenous human biomarkers that can be measured  
115 directly in wastewater samples have been evaluated to estimate their human fecal content. These  
116 markers include but are not limited to: (1) bacteria/viruses or molecules that are ubiquitous in  
117 human intestinal tracts, such as cross-assembly phage, human ribonuclease P,<sup>17</sup> and *Bacteroides*  
118 HF183;<sup>18</sup> (2) an exogenous substance (or its' metabolite) after intentional consumption of a  
119 substance (i.e., personal care products, food additives and dietary supplements such as  
120 carbamazepine and gabapentin,<sup>19</sup> artificial sweeteners,<sup>20</sup> and caffeine and its metabolite  
121 (paraxanthine),<sup>10</sup> pepper mild mottle virus (PMMoV);<sup>18</sup> and (3) endogenous compounds that are  
122 produced naturally in the body such as creatinine, cholesterol and its metabolite coprostanol,  
123 cortisol, and serotonin metabolite 5-hydroxyindoleacetic acid (5-HIAA).<sup>11</sup>

124 Pepper mild mottle virus (PMMoV), a virus ingested with pepper-containing food, has been  
125 widely measured and frequently used for normalizing SARS-CoV-2 concentration data. The  
126 PMMoV is one of the widely used normalization biomarkers in wastewater SARS-CoV-2  
127 surveillance because it is believed to be present in high concentrations in wastewater, introduced  
128 into the human body through the diet, and has the potential to serve as an RNA recovery control  
129 since it is a single-stranded RNA virus.<sup>21,22</sup> D'Aoust et al. found PMMoV to be superior to  
130 HF183 *Bacteroides* 16S ribosomal rRNA and eukaryotic 18S rRNA, as PMMoV showed more  
131 reproducibility within and between WWTPs<sup>18</sup>. Creatinine, the endogenous nitrogenous waste  
132 product, has been used to normalize the concentrations of other urinary excretion products to  
133 account for urine dilution in clinical chemistry and is recommended as a possible biomarker for  
134 estimating the population.<sup>23</sup> The serotonin metabolite, 5-HIAA, has also been evaluated as a  
135 wastewater marker, and was reported to be more stable within sewer systems than cortisol and  
136 androstenedione.<sup>24</sup>

137 Caffeine (1,3,7-trimethylxanthine) is one of the world's most widely consumed dietary  
138 ingredients, found in many globally popular products, including tea, cola and energy drinks, and  
139 in some medications and nutritional supplements. Still, the most important source of this alkaloid  
140 is coffee.<sup>25</sup> The excretion of the metabolite of caffeine, paraxanthine (1,7-dimethylxanthine), was  
141 less affected by the genetic-based variation in pharmacokinetics than the parent compound was,  
142 therefore, suggested as a potential biomarker for dietary caffeine intake.<sup>26</sup> Chemicals (e.g.,  
143 paraxanthine) involved in endogenous metabolism (products of biosynthesis or catabolism) avoid  
144 xenobiotics' problems for use as proxy measures for population since their association with per  
145 capita activities has higher fidelity.<sup>23</sup> Caffeine and paraxanthine are easy to detect due to the high  
146 concentration levels ( $\mu\text{g/L}$ ) in untreated wastewater,<sup>27</sup> and are stable in wastewater samples

147 stored at 4°C,<sup>28</sup> which makes them ideal biomarkers. However, more research was needed for  
148 caffeine and paraxanthine application in the concept of WBE.

149 In a previous study, we compared five biomarkers, PMMoV, creatinine, 5-HIAA, caffeine,  
150 and paraxanthine, based on two weeks' data, for their utility in normalizing SARS-CoV-2 loads  
151 and found caffeine and especially paraxanthine were the most reliable population biomarkers.<sup>29</sup>  
152 This study extended the investigation to the long-term weekly monitoring of 64 wastewater  
153 treatment plants (WWTPs) across Missouri for more than six months to compare the utility of  
154 caffeine, paraxanthine, and PMMoV as population biomarkers across seasons and distinct  
155 geographical areas with contrasting sewershed sizes.

## 156 **2. MATERIALS AND METHODS**

### 157 **2.1 Wastewater sampling and clinical COVID-19 case**

158 Triplicates of 50 mL of 24-hr composite influent (before primary treatment) samples were  
159 collected once per week from 64 WWTPs in Missouri (Fig. 1), and a total of 41 weeks from May  
160 2021 to April 2022 (weeks of 05/10/2021, 05/24/2021, 06/28/2021, and consecutively from  
161 weeks of 07/19/2021 to 04/10/2022). A majority of samples were collected as 24-hr time-  
162 proportional composites and only 6 WWTPs were collected as 24-hr flow-proportional  
163 composites. Each WWTP collected samples on the same day of the week during the study  
164 period. The first half of the sampling period was dominated by the Delta variant, and the second  
165 half was dominated by the Omicron variant. In total, 2624 wastewater samples were collected.

166 Wastewater samples were transported in insulated shippers with ice packs to the University  
167 of Missouri within 24 hr from the collection and then stored at 4°C until extraction. WWTPs  
168 reported their 24-hr flow rates and weekly new COVID-19 cases were provided by the Missouri  
169 Department of Health and Senior Services (DHSS). Weekly clinical COVID-19 cases for each  
170 WWTP service area were obtained by matching clinically confirmed COVID-19 case data  
171 (georeferenced using home address) to WWTPs sewershed boundaries in ArcGIS. Sewershed  
172 boundaries were either provided by the municipality or, in many cases (12 WWTPs), the  
173 municipality did not have geospatial data delineating their sewershed boundaries, so municipal  
174 boundaries were used to approximate a service area.

175 The 64 WWTPs cover urban, semirural, and rural locations throughout Missouri with the  
176 sewershed population ranging from 900 to 490,000. Sewershed size (metadata population) was  
177 either provided by the WWTP or estimated based on the number of residential connections  
178 reported in a WWTP's discharge permit and the average household size for that municipality  
179 from the most recent U.S. Census at the time the facility began sampling. Based on the  
180 population served by the 64 WWTPs, there is the potential to monitor 50% of the 6.15 million  
181 Missouri population.<sup>30</sup> A summary of each facility, including the population served and the  
182 locations, is provided in Table S1. Additionally, ten wastewater composite samples collected  
183 from WWTPs in Wisconsin during the week of 06/07/2021 were utilized as a data set for model  
184 evaluation and validation.



## 185 **2.2 Mobility data**

186 Daily data on mobility (driving and walking) were downloaded for Columbia, MO,  
187 between 01/13/2020 and 04/13/2022 from Apple Mobility Trends Reports<sup>31</sup>. Apple mobility data  
188 has no demographic information about the users. The original mobility indices were relative  
189 percentages to the reference date on 01/13/20, which were scaled to the maximum observed  
190 during the study period.

## 191 **2.3. Wastewater concentrations of caffeine and paraxanthine.**

### 192 ***2.3.1. Extraction of caffeine and paraxanthine***

193 For all 2,624 wastewater samples, 1.5 ml was centrifuged at 10000 rpm for 10 minutes, and  
194 0.75 ml supernatant was extracted and mixed with 0.75 ml ammonium acetate buffer (10 mM  
195 ammonium acetate and 0.1% formic acid in water). Then, 10  $\mu$ L of formic acid was added to  
196 precipitate the large molecules in the wastewater, followed by spiking Caffeine-C<sup>13</sup> to evaluate  
197 the recovery of endogenous caffeine. For improved sample storage stability, the 0.75 ml  
198 ammonium acetate buffer was replaced by 0.75 ml 100% methanol starting from December  
199 2021. The two preparation methods (ammonium acetate buffer and methanol) were compared,  
200 and no significant difference in caffeine and paraxanthine concentrations was found before the  
201 transition (Table S2). Finally, the mixture was filtered through 0.2  $\mu$ m PTFE filters (13mm)  
202 (Waters, USA) before the liquid chromatography with tandem mass spectrometry (LC-MS/MS)  
203 analysis.

### 204 ***2.3.2. Liquid chromatography-tendon mass spectrometry analysis.***

205 The quantification of caffeine and paraxanthine was performed on a Waters Alliance 2695  
206 High Performance Liquid Chromatography (HPLC) system coupled with Waters Acquity TQ  
207 triple quadrupole mass spectrometer (MS/MS). The analytes were separated on a Phenomenex  
208 (Torrance, CA) Kinetex C18 (100mm x 4.6 mm; 2.6  $\mu$ m particle size) reverse-phase column.  
209 The mobile phase consisted of 10 mM ammonium acetate and 0.1% formic acid in water (A) and  
210 100% acetonitrile (B). The gradient conditions were 0 – 0.3 min, 2% B; 0.3-7.27 min, 2-80% B;  
211 7.27-7.37 min, 80-98% B; 7.37-9.0 min, 98% B; 9-10 min 98-2% B; 10.0 – 15.0 min, 2% B at a  
212 flow rate of 0.5 mL/min. The ion source in the MS/MS system was electrospray ionization (E.I.)  
213 operated in positive ion mode with a capillary voltage of 1.5 kV. The temperature of the  
214 ionization source was 150°C, and that of the desolvation zone, 450°C. The optimized collision  
215 energy, cone voltage, and molecular and product ions of the biomarkers are summarized in Table  
216 1.

## 217 **2.4.1 Wastewater concentrations of SARS-CoV-2 and PMMoV**

### 218 ***2.4.1. RNA extraction***

219 Samples from the weeks of 09/13/2021 to 04/10/2022 were processed for both SARS-CoV-2  
220 and PMMoV quantification. First, 50-ml raw wastewater samples were spun at 2000  $\times$ g for 5  
221 min to remove large particulates, then vacuum filtered through a 0.22  $\mu$ m filter (Millipore cat#  
222 SCGPOO525). Then, 35.5 mL of filtered wastewater was mixed with 12 mL of 50% (W/V)

223 polyethylene glycol (PEG, Research Products International, cat# P48080) and 1.2M NaCl,  
224 followed by equilibration for 2 h at 4°C, all done on the day of sample receipt. Afterwards,  
225 samples were centrifuged at 12,000 x g for 2 h. RNA was extracted from the pellet using the  
226 Qiagen Viral RNA extraction kit following the manufacturer's instructions after removing the  
227 supernatant. RNA was eluted in a final volume of 56 µL and stored at -80°C if it was not  
228 processed immediately.

#### 229 **2.4.2. RT-qPCR**

230 The extracted RNA was used to perform RT-qPCR quantification of the genetic material of  
231 SARS-CoV-2 and PMMoV, separately. SARS-CoV-2 was quantified using the primer and  
232 control sets described in Robinson et al.,<sup>32</sup> and PMMoV was quantified using the primer sets  
233 described in Hsu et al.<sup>29</sup> A plasmid carrying a PMMoV gene along with an N gene fragment was  
234 constructed, purified from *Escherichia coli*, and used as standards for the RT-qPCR assay. Final  
235 RT-qPCR one-step mixtures consisted of 5 µL TaqPath 1-step RT-qPCR Master Mix (Thermo  
236 Fisher), 500 nM of each primer, 125 nM of each TaqMan probes, 5 µl of wastewater RNA  
237 extract, and RNase/DNase-free water to reach a final volume of 20 µL. All RT-qPCR assays  
238 were run in duplicate on a 7500 Fast real-time qPCR instrument (Applied Biosystems). The  
239 reactions were initiated with one cycle of UNG incubation at 25°C for 2 min and then one cycle  
240 of reverse transcription at 50°C for 15 min, followed by one cycle of activation of DNA  
241 polymerase at 95°C for 2 min and then 45 cycles of 95°C for 3 sec for DNA denaturation and  
242 55°C for 30 sec for annealing and extension. The data would be collected at the step of 55°C  
243 extensions. The concentration of SARS-CoV-2 and PMMoV genomes in each sample,  
244  $[N1.N2]_{SARS}$  or  $[PMMoV]$  (copies/L), was calculated using Eq. 1.

$$245 \quad [N1.N2]_{SARS} \text{ or } [PMMoV] = N / (V_{RT-qPCR} \times (V_{sample} / (V_{extracted}/\text{recovery rate}))) \quad (1)$$

246 where N (copies/reaction) is the gene copies detected in each RT-qPCR reaction,  $V_{RT-qPCR}$  is the  
247 volume of RNA used for RT-qPCR (5 µL),  $V_{sample}$  is the wastewater sample volume initially  
248 used for the concentration step (35.5 mL), and  $V_{extracted}$  is the total volume of nucleic acid  
249 extracted (56 µL).

### 250 **2.5 Statistical analyses**

251 The statistical analyses included the following three steps: 1) estimation of the real-time  
252 population using the wastewater biomarker mass loads; 2) population normalization for  
253 wastewater SARS-CoV-2 viral load and COVID-19 case to wastewater SARS-CoV-2 viral  
254 concentration (copies/week/10,000 people) and COVID-19 incidence rate (case/week/10,000  
255 people), and 3) comparison of the strength of the relationships between population normalized  
256 wastewater SARS-CoV-2 viral load and COVID-19 incidence rate under different normalization  
257 scenarios.

#### 258 **2.5.1. Real-time population estimation using wastewater biomarker loads**

259 All the data analyses were conducted using the R program.<sup>33</sup> To compare biomarkers'  
260 variability and temporal consistency, the coefficient of variation (CV%) of the three biomarkers  
261 across seven months of data at each of the 64 WWTPs was calculated. Only 7-months of data

262 (n=1596) between the weeks of 09/13/2021 to 04/10/2022 were included in the analyses to  
263 compare three biomarkers since PMMoV was only measured after 09/13/2021. The relationship  
264 between weekly biomarker load and the population contributing to the wastewater was examined  
265 using linear regression. The biomarker load of biomarker  $i$  for  $j$  WWTP,  $B_{ij}$ , was calculated as

$$266 \quad B_{ij} = [B]_{ij} \times F_j \times 7 \times 3.7841 \times 10^6 \quad (2)$$

267 in which  $[B]_{ij}$ , the biomarker  $i$  concentration in  $j$  WWTP wastewater sewershed, was determined  
268 by LC-MSMS or RT-qPCR.  $F_j$  is the wastewater daily flow volume (million gallons per day) for  
269 WWTP $_j$ . Constants 3.78541 and 7 are applied to convert the imperial unit to metric unit and  
270 daily to weekly biomarker load, respectively.

271 The linear regression model was conducted as

$$272 \quad B_i = \beta_i P + \epsilon_i \quad (3)$$

273 Where  $P$  is the corresponding population from metadata data. The modeling was based on the  
274 assumption that the mass load entering the treatment plant per day of a chemical is proportional  
275 to the contributing population. Since the actual real-time population was not available, the best  
276 estimation of it was the metadata population.  $B_i$  is the biomarker mass load,  $\epsilon_i$  the error term, and  
277  $\beta_i$  the estimated parameter for biomarker  $i$ . Log transformation was applied to the population and  
278 biomarker load.

279 In addition, ten wastewater samples (each from different WWTFs) from Wisconsin collected  
280 during the week of 06/07/2021 were used to validate equations (3) using Root Mean Square  
281 Error (RMSE). The RMSE is the standard deviation of the prediction errors.

282 Then, the real-time population  $P_{RT}$  by biomarker  $i$  was estimated using all three biomarkers  
283 according to the equation

$$284 \quad P_{RTi} = (B_i - \epsilon_i) / \beta_i \quad (4)$$

### 285 **2.5.2. Population normalization of wastewater SARS-CoV-2 load and COVID-19 incidence** 286 **rate.**

287 Wastewater SARS-CoV-2 load was then normalized to population (copies/week/10,000  
288 people) by dividing the SARS-CoV-2 load per week by each of the three estimated population  
289 metrics:

$$290 \quad \text{Normalized [SARS-CoV-2]}_i = \frac{[N1.N2]_{SARS} \times (F_j \times 3.7841 \times 10^6) \times 7 \times 10000}{\text{Real-time Population}_i \text{ or } P_{\text{metadata}}} \quad (5)$$

291 in which  $[N1.N2]_{SARS}$  (copies/L), the SARS-CoV-2 concentration in the wastewater sewershed,  
292 was determined by RT-qPCR using equation (1). The COVID-19 incidence rate was defined as:

$$294 \quad \text{Normalized Covid-19 incidence rate}_i = \frac{\text{Clinic case number} \times 10000}{\text{Real-time Population}_i \text{ or } P_{\text{metadata}}} \quad (6)$$

295 Population normalization better allows the results to be compared across WWTPs that serve  
296 different size populations.



### 297 **2.5.3. Effectiveness of population normalization on the relationships between wastewater** 298 **SARS-CoV-2 load and clinical COVID-19 incidence rate.**

299 To compare the outcomes of population normalization of different biomarkers, the strength  
300 of the linear regression models from normalized wastewater SARS-CoV-2 load to normalized  
301 COVID-19 incidence rate were compared across markers, as well as when there was no  
302 population normalization (i.e., the correlation strength of raw viral load per week with total case  
303 number per week). Specifically, the goodness of fit of linear regression models was compared  
304 within each WWTP using the coefficient of determination ( $R^2$ ), the measure of “variance  
305 explained”. Analysis of variance (ANOVA) and pairwise comparisons were conducted on the  $R^2$   
306 of four groups (without normalization, metadata population normalization, caffeine estimated  
307 population normalization, paraxanthine estimated population normalization, and PMMoV  
308 estimated population normalization) within each WWTP. Log transformation was applied to both  
309 wastewater SARS-CoV-2 load and the COVID-19 incidence rate. Since there are many “0”  
310 COVID-19 cases,  $\log_{10}(x+1)$  was employed for the COVID-19 incidence rate.

## 311 **3. RESULTS**

### 312 **3.1. Temporal variations of biomarkers**

313 The coefficient of variations (CV%) of the three biomarkers across seasons at each of the  
314 64 WWTPs was calculated (Fig. 2). The mean CV% across all the facilities were not different  
315 between caffeine (43%) and paraxanthine (40%), but both significantly lower than the CV% of  
316 PMMoV (mean=67%) ( $p<0.001$ ). Paraxanthine was the only biomarker with all the CV% lower  
317 than 100% and the smallest range of CV% among 64 WWTPs (caffeine = 263%, paraxanthine =  
318 54%, and PMMoV = 154%). The lower CV% means of caffeine and paraxanthine than PMMoV  
319 indicated that caffeine and paraxanthine changed less over time than PMMoV. No significant  
320 relationship between each biomarker’s CV% and population size was found (data not shown).  
321 Compared to caffeine and PMMoV, the smallest CV% range of paraxanthine among WWTPs  
322 showed paraxanthine is less influenced by population attributes (i.e., population size, the  
323 composition of age, race, and ethnicity, and environmental factors such as season and fecal  
324 strength across geographic regions).

325 The outlier of CV% of caffeine (280%) was the Sikeston Wastewater Treatment Plant  
326 (SKSTN), which is nearby a global industry factory, Unilever ice cream, manufacturing the  
327 distributed worldwide Magnum chocolate ice cream bar (caffeine concentration in chocolate is  
328 around 420  $\mu\text{g/g}$ ). Eleven out of 16 samples with caffeine concentrations over 200  $\mu\text{g/L/week}$   
329 were from SKSTN. The extreme caffeine concentrations were not likely all shed by humans  
330 from such a small town with a population of 17,000 but rather from industrial waste. After  
331 removing samples from SKSTN, there was a strong linear relationship between caffeine and  
332 paraxanthine concentration (Fig. S1). Therefore, caffeine is still a reliable biomarker for the area  
333 where no such exogenous caffeine sources exist.

### 334 **3.2. Real-time population prediction by biomarkers**

335 Linear regression models were established for biomarker mass load per week and  
336 population sizes obtained from the metadata for both Missouri. Then, real-time population ( $P_{RT}$ )

337 was predicted for each WWTP with all available data. The estimated  $P_{RT}$  of tourism town  
338 (ANON2) from all three biomarkers was generally higher than the metadata population, which is  
339 reasonable since the metadata population primarily only counts residents. The estimated  $P_{RT}$  for  
340 the large metropolitan area, Kansas City Blue River, was almost always lower than the metadata  
341 population (Fig. S3A), probably indicating a population decline in the past two years since the  
342 census survey in 2020. There was a strong relationship between the metadata population and the  
343 total case number during the seven months from 09/13/2021 to 04/10/2022 (Fig. S3B and S3C).  
344 Kansas City Blue River was the “outlier” in Fig S3B, suggesting that the PRT of the Kansas City  
345 Blue River area might be substantially lower than the metadata population. Upon further  
346 investigation, it was learned that KCBLU WWTP was in the process of upgrading and the served  
347 area changed periodically compared to the metadata population that the facility initially provided  
348 (personal communication).

349 Therefore, models between biomarker mass load and population were revised by  
350 removing KCBLU WWTP in the models for Missouri (Fig. 3A, 3C, 3E) and metadata  
351 normalization data in KCBLU were also removed in the following analyses. Linear regression  
352 models were also established for biomarker mass load per week and population sizes obtained  
353 from the metadata for Wisconsin (Fig. 3B, 3D, 3F). Within Missouri, the model with  
354 paraxanthine had the highest  $R^2$  among all three biomarkers. Similar trends were observed in  
355 Wisconsin models, especially the paraxanthine model, which confirmed that the relationship  
356 between biomarkers and population could be applied beyond Missouri. In addition, Wisconsin  
357 samples were used to test Missouri models (Fig. 3A, 3C, 3E) using RMSE, which were 0.24,  
358 0.19, and 0.87 for models of caffeine, paraxanthine, and PMMoV. The lowest RMSE of the  
359 paraxanthine model indicated it is the best predictor of the population too.

360 The ratios of the estimated real-time population to the metadata population ( $P_{RT}$   
361  $/P_{METADATA}$ ) by paraxanthine had the smallest mean and standard deviation among the 64  
362 WWTPs (Table 2). Among the three biomarkers, caffeine and paraxanthine, in general, are  
363 closer to the metadata populations. In contrast, estimated  $P_{RT}$  from PMMoV wavered with time  
364 dramatically. The smaller variations of estimated  $P_{RT}$  from caffeine and paraxanthine than  
365 PMMoV are consistent with the low temporal variations of caffeine and paraxanthine relative to  
366 PMMoV.

367 A case study of validation of biomarker population estimation using the Apple mobility  
368 data was conducted in a college town, Columbia, Missouri. The Apple mobility showed that  
369 demographic migration was influenced by the COVID-19 pandemic and the school events in  
370 Columbia, Missouri (Fig. 4A). For instance, there was a sharp decline of mobility in April 2020  
371 after the Missouri “Stay home” order. Both mobility data and the estimated  $P_{RT}$  estimated by  
372 paraxanthine showed the fluctuations of the population with school semesters and holidays (Fig.  
373 4A and B). For instance, Labor Day weekend, Thanksgiving break, and winter break had lower  
374  $P_{RT}$  and mobility than other times since a large group of students traveled back to their  
375 hometowns during these holidays. Also, the week of the University of Missouri Homecoming  
376 event (10/05/2021) had a  $P_{RT}$  and mobility increase.

### 377 3.3. Effectiveness of population normalization of different wastewater biomarkers

378 The strengths of the relationships between the population normalized SARS-CoV-2 RNA  
379 load and COVID-19 incidence rate were compared within each WWTP (Table 3). A total of 59  
380 out of 64 WWTPs showed a significant positive relationship between wastewater SARS-CoV-2  
381 RNA load and clinical COVID-19 incidence rate for all population normalization scenarios. In  
382 addition, models were significant except for the PMMoV estimated population normalization  
383 model for two WWTPs (ANON1 and MACON). Within 57 of 64 WWTPs, biomarker  
384 normalizations strengthened the relationship between SARS-CoV-2 RNA load and normalized  
385 COVID-19 incidence rate (i.e.,  $R^2$  increased). The mean  $R^2$  decreased ( $\alpha$  level=0.1) in the order:  
386 paraxanthine estimated real-time population normalization > without population normalization  
387 and metadata population normalization > caffeine estimated real-time population  
388 normalization > PMMoV estimated real-time population normalization, indicating that  
389 paraxanthine is the best population normalization biomarker (Fig. S3).

390 The regression models of viral loads with clinical incidence after normalization to  
391 paraxanthine estimated population had the highest  $R^2$  among all five models for 40 out of 61  
392 WWTPs (Fig. 5). In contrast, the strength of the relationship between wastewater viral load and  
393 clinical incidence after PMMoV and caffeine estimated population normalization became weaker  
394 than without population normalization or with metadata population normalization (Fig. S3).  
395 Therefore, the time series of wastewater viral load and COVID-19 incidence rate with  
396 normalization of paraxanthine estimated population was plotted for each WWTP (Fig. 6).  
397 Weekly wastewater viral copies followed similar patterns with clinical incidence rates for most  
398 WWTPs. Furthermore, the strength of the relationship between wastewater SARS-CoV-2 viral  
399 load and the COVID-19 incidence rate was significantly increased with increasing cases and  
400 metadata population (Fig. 7A and 7B).

### 401 3.4. Limit of detection of wastewater SARS-CoV-2 surveillance

402 The linear regression relationship between wastewater SARS-CoV-2 RNA load with clinical  
403 cases was tested for models without population normalization and paraxanthine population  
404 normalization (Fig. S4). According to the paraxanthine population normalization model, the  
405 process limit of detection (PLOD) (entire process from the sampling to the analysis of RT-qPCR)  
406 in the wastewater over should be:

$$407 \quad PLOD1 \text{ (copy/week)} = 1.3 \times 10^{11} \quad (7)$$

408 A validation calculation was conducted using the PLOD (<3,954 GC/50ml; 95% probability of  
409 detection) of the US CDC N1 RT-dPCR and RT-qPCR assays from a study based on wastewater  
410 SARS-CoV-2 seeding experiment by Ahmed et al.<sup>34</sup> (Table 4):

$$411 \quad PLOD2 \text{ (copy/week)} = (3,954 \text{ copy/50 ml}) \times 1000 \text{ ml} \times F_i \times 3.7841 \times 10^6 \quad (8)$$

412 Although Ahmed et al. used a different adsorption extraction method of virus to evaluate N1  
413 copy instead of average copy of N1 and N2 as in this study, both PLOD1 and PLOD2 showed  
414 that the N1N2 mass load was higher than PLODs for ANON1 (the smallest WWTP) during the  
415 three weeks when the main outbreak occurred. The PLOD1 was likely higher than the actual

416 value since the clinical cases are likely less than the real cases due to the asymptomatic and  
417 underreported cases.

## 418 **4. DISCUSSION**

### 419 **4.1 Paraxanthine was the optimal population biomarker**

420 The reduced strength of the relationship between the PMMoV-population normalized SARS-  
421 CoV-2 load and COVID-19 incidence rate was consistent with previous studies that showed  
422 PMMoV had mixed or adverse effects on the correlation between wastewater measurements of  
423 SARS-CoV-2 and clinical cases.<sup>35-37</sup> To the best of our knowledge, there is only one nationwide  
424 study to date (conducted by Biobot Analytics) that is comparable with our study in terms of the  
425 temporal and spatial magnitudes of sampling. That study collected 2,433 samples from 55  
426 WWTPs across the U.S. and found that PMMoV normalization did not always improve the  
427 correlation between wastewater measurement and clinical cases.<sup>35</sup> Feng et al. showed that  
428 PMMoV normalizations reduced the correlations between SARS-CoV-2 concentration and  
429 COVID-19 incidence for 8 of 12 WWTPs and suggested that variability's influence across  
430 measurement for human viral is stronger than that of differences in the fecal loads in the  
431 samples<sup>36</sup>. For some sewersheds where the normalizations by metadata population and without  
432 population normalization were better than the normalizations by caffeine and PMMoV estimated  
433 population, probably because most WWTPs serve rural areas in Missouri where the population  
434 does not fluctuate with time. However, each WWTP was weighted equally in this analysis  
435 regardless of the population size it serves. Furthermore, many people worked from home during  
436 the pandemic; therefore, the real-time population was expected to be closer than usual to the  
437 metadata population for many regions.

438 The intensified relationship between wastewater SARS-CoV-2 viral load with clinical  
439 COVID-19 cases by wastewater paraxanthine concentration for 2/3 of the WWTPs and the  
440 consistency of the relationship between wastewater paraxanthine concentration and population  
441 between Missouri and Wisconsin demonstrated that paraxanthine is a reliable population  
442 biomarker across large geographical regions with different sizes of the population. The superior  
443 performance of paraxanthine over PMMoV could be attributed to its 1) much longer half-life, 2)  
444 less exogenous sources and variability of excretion rate intra-individual and inter-individual, 3)  
445 easier and more accurately determined in the wastewater.

#### 446 **4.1.1 Stability**

447 A promising population normalization biomarker should be stable in wastewater.  
448 Caffeine and its metabolites in untreated wastewater were stable during 24 hr storage at 4°C and  
449 20°C and also stable at -20°C for up to four weeks.<sup>28</sup> One study showed PMMoV was stable for  
450 21 days at 4°C, 25°C, and 37°C,<sup>38</sup> However, it was mostly based on different water types that had  
451 simpler contents than wastewater, such as deionized water and autoclaved wetland water. In  
452 addition, the conclusion that PMMoV has high stability over time was drawn from much shorter  
453 periods of investigations or a small number of samples collected from fewer WWTPs than in our  
454 study<sup>4,18,21,22,36</sup>. For instance, a highly cited article from Kitajima et al. found that PMMoV did  
455 not change seasonally, but was only based on 48 samples collected from two WWTPs over 12  
456 months.<sup>21</sup> Wu et al. only tested PMMoV stability for SARS-CoV-2 fecal biomarker on samples

457 collected over one week during March 2020.<sup>4</sup> D’Aoust et al. found that PMMoV is a better  
458 normalization biomarker than *Bacteroides* 16S rRNA or human 18S rRNA, which was also only  
459 based on 23 samples from two WWTPs.<sup>18</sup> In contrast, higher stability of paraxanthine than  
460 PMMoV in our study was based on 1569 samples from September 2021 to April 2022, which  
461 covered three months of the Delta variant in 2021 and the major spike of the Omicron variant at  
462 the beginning of 2022. The 64 WWTPs represent 50% of the entire Missouri population, from  
463 metropolitan areas such as St. Louis to small rural towns with only 900 people.

#### 464 **4.1.2. Sources**

465 A reliable population biomarker should primarily be shed by humans and respond to the  
466 population size, not environmental factors.<sup>8</sup> A regular and constant consumption is a further  
467 prerequisite for a good marker.<sup>39</sup> Loads of caffeine in untreated wastewater reflect not only  
468 consumption, metabolism, and excretion of the compound but also caffeine from beverages,  
469 foods, and pharmacologic that were poured out directly.<sup>40</sup> Caffeine is transformed in the human  
470 liver into more than 20 metabolites, primarily dimethylxanthines (paraxanthine, theobromine,  
471 and theophylline), dimethyl- and monomethyluric acids, and uracil derivatives<sup>39</sup>. Between 0.5%  
472 and 10% of the caffeine in human body is excreted unmetabolized via urine.<sup>39</sup> Exogenous  
473 sources from industrial wastewater can influence caffeine if the WWTP is a combined sewer  
474 system, which also has potential pollution issues from the outflow.<sup>7</sup> Besides, we also had several  
475 samples that could not detect caffeine and paraxanthine after heavy storms (data removed from  
476 analyses). Therefore, if combined sewer systems are chosen for WWTP, individuals should be  
477 aware that in some circumstances, like high rain events, readings of viral load and other  
478 measurements may need be corrected for dilution.

479 As a caffeine metabolite, paraxanthine mainly comes from human metabolism.<sup>8</sup> Therefore,  
480 paraxanthine relates to the population better than caffeine. Among the metabolites of caffeine,  
481 paraxanthine is the most abundant caffeine metabolite in wastewater.<sup>26</sup> In addition, 1-  
482 methylxanthine, 7-methylxanthine, and 1,7dimethyluric acid are also metabolites of theophylline  
483 and theobromine respectively, which are present in some foods, drinks, and pharmaceutical  
484 formulations.<sup>39</sup> Paraxanthine was believed to be the optimal biomarker of caffeine intake as a  
485 population biomarker.<sup>1</sup> The more minor variations of paraxanthine among different WWTPs  
486 were probably due to similar levels of caffeine intake among different groups in the population.  
487 The main factor driving paraxanthine load in the wastewater was the coffee consumption rate,  
488 which can be influenced by the composition of the population age since kids do not drink as  
489 much as adults. In addition, average consumption is 70 mg per person per day but varies in the  
490 different countries due to the different culture.<sup>39</sup> However, caffeine is one of the most widely  
491 consumed dietary ingredients worldwide, and thus paraxanthine as its metabolite has the  
492 potential to be used as a population biomarker worldwide.

493 In comparison, PMMoV is a pepper pathogen virus that often is found in human feces, as  
494 well as peppers and processed pepper products from all over the world, such as dry spices and  
495 sauces.<sup>42</sup> Unlike caffeine or tea are widely consumed by people all over the world, the  
496 importance of pepper in cuisine varies depending on the regions. For example, chili pepper is the  
497 defining ingredient of New Mexican food but not for most European cuisine. Therefore, the  
498 population race composition might influence the pepper’s consumption and thus PMMoV  
499 concentration. The detection level of PMMoV in human feces varies greatly from 7% to 95%,



500 depending on the study's regions and also between adults and children, even in the same  
501 regions.<sup>43</sup> The PMMoV concentration in our study had an average of  $1.5 \times 10^8$  copy/L, which is  
502 consistent with the previous study that showed the PMMoV concentration from raw wastewater  
503 ranged from  $10^8$ - $10^{10}$  copy/L,<sup>44</sup> but PMMoV in our study largely ranged from  $3 \times 10^4$  to  $2 \times 10^9$   
504 copy/L.

505 In addition, SARS-CoV-2 RNA and PMMoV are shed in fecal, but caffeine and paraxanthine  
506 are discharged through urine. Humans urinate much more frequently than bowel movement, likely  
507 contributing to less variance in quantity among individuals than bowel movement, which  
508 possibly is one of the reasons that biomarkers in urine such as caffeine and paraxanthine had less  
509 variations and are more representative of population size.

### 510 **4.1.3. Quantification**

511 Being easy to be determined with high repeatability is another criterion of a good population  
512 marker. The low variation of caffeine and paraxanthine owes to the high analytical sensitivity of  
513 LC-MSMS system and the consistent and high extraction recovery rate. With the development of  
514 technology, most of LC-MSMS systems have ng/mL to pg/mL level sensitivity. The instrumental  
515 detection limits for caffeine and paraxanthine were reported as 1.4 and 2.4 pg/injected, and  
516 instrumental quantification limits for caffeine and paraxanthine were 3.6 and 6.6 ng/L using  
517 API5500 QqQ equipped with a Turbo Ion Spray source.<sup>28</sup> The sensitivity of our HPCL-MSMS  
518 with electrospray ionization is at ng/mL, but it is sufficient for wastewater caffeine and  
519 paraxanthine quantification. The caffeine concentration in wastewater influent water was  
520 reported from 20-300 µg/L (Canada), 20 µg/L (U.S.), and  $147 \pm 76$  µg/L (Germany).<sup>28</sup> In our  
521 study, the average caffeine and paraxanthine concentrations were 71 µg/L and 17.5 µg/L,  
522 respectively. The recoveries of caffeine and paraxanthine from untreated wastewater were 88%  
523 and 76% during the similar storage temperature and extraction method to our study.<sup>28</sup> Our  
524 previous study showed that the recovery rates of caffeine and paraxanthine during injection are  
525  $101 \pm 7\%$  and  $92 \pm 3\%$ .<sup>29</sup> In addition, the repeatability for caffeine and paraxanthine was quite high  
526 (CV%: 12% and 5%).<sup>28</sup>

527 Unlike the simple chemical analysis on LC-MSMS, PMMoV measurement has a very  
528 complex workflow. First, wastewater samples require the application of concentration steps  
529 before extraction of the RNA fragments. Then, highly-sensitive molecular assays using RT-  
530 qPCR or RT-dPCR (digital PCR) will be applied to quantify the PMMoV concentration.<sup>34</sup>  
531 Consequently, there are many factors that may contribute to the large variation, such as the  
532 efficiency of primary concentration, loss through nucleic acid extraction, and inhibition of  
533 reverse transcription or PCR amplification. PMMoV's recovery rates reported in previous studies  
534 varied but were generally lower than caffeine and paraxanthine (e.g.,  $45 \pm 26\%$  using direct  
535 extraction and only  $>10\%$  using electronegative (H.A.) filters).<sup>36,45</sup> The recovery rate of PMMoV  
536 in this study was not tested directly, but the virus concentration methods (PEG concentration) in  
537 this study preserved SARS-CoV-2 N1N2 at approximately 62% signal on average and 2.7 times  
538 higher for Puro.<sup>32</sup> The PMMoV's process limits of quantification and detection were evaluated in  
539 diluted wastewater in the coastal water,<sup>46</sup> which is different from PMMoV in raw wastewater.

## 540 4.2 Normalization approach recommendation for SARS-CoV-2 wastewater-based 541 epidemiology

542 A previous study showed that outbreaks could be detected in buildings with as many as 1,000  
543 occupants.<sup>47</sup> This study showed that the wastewater could also detect community-level outbreaks  
544 with a small population size, which revealed that the process limit of detection for wastewater  
545 surveillance (e.g., the fewest infections in a community that can be reliably detected in  
546 wastewater) is quite low (~0.1% of the population, 1-2 cases in 900) (Table 4). However, the  
547 PLOD could be overestimated since the actual cases could be higher than just 1 or 2 cases. The  
548 smallest WWTP, ANON1, still showed a significant relationship between the wastewater viral  
549 copies and the COVID-19 incidence rate, except when using the normalization of PMMoV  
550 estimated population (Table 3). Our previous study found that approximately 20% of the tested  
551 WWTPs in Missouri, U.S., receive some input from industries, possibly discharging some  
552 chemicals that suppress the viral signals in wastewater.<sup>48</sup> MACON WWTP was one of the  
553 examples.<sup>48</sup> However, positive relationship between the wastewater viral load and the COVID-  
554 19 incidence rate for MACON except for PMMoV estimated population normalization (Table 3).  
555 Therefore, WBE is a feasible approach for population-level monitoring of COVID-19 disease.  
556 PMMoV, however, is not an ideal population biomarker, especially for small towns due to its  
557 large temporal variation.

558 Many wastewater SARS-CoV-2 surveillance studies have been conducted across the U.S.  
559 during the last two years<sup>35</sup>, which provided an excellent network for the effective and long-term  
560 monitoring of SARS-CoV-2 and possibly other diseases in the future. Thus far, however, the  
561 normalization applied to the SARS-CoV-2 wastewater surveillance does not have a standardized  
562 approach. There are three main types of normalization: 1) normalized to WWTP flow (e.g.,  
563 copies/week, to give viral load), 2) normalized to WWTP human fecal biomarker estimated  
564 population (e.g., copies/10K people/week), and 3) directly normalized to WWTP human fecal  
565 biomarker loads (e.g., copies/copy of PMMoV/week).

566 Wastewater flow normalization converts the measured viral concentration to viral load,  
567 accounting for variations in flow between days due to precipitation, snowmelt, or groundwater  
568 inflow. Established on the flow normalization, the normalization to biomarker estimated  
569 population evaluated in this study aims to account for the variations caused by wastewater  
570 volume and population size that contribute to the waste. The third normalization is used often  
571 because it does not involve wastewater volume and population information. However, it is based  
572 on the assumption that the measured wastewater biomarker concentration perfectly reflects the  
573 population dynamics. Many previous studies used PMMoV as SARS-CoV-2 internal control to  
574 normalize SARS-CoV-2 concentration to SARS-CoV-2 copies per copy of PMMoV.<sup>4,18,49</sup>  
575 However, our study showed that the relationship between PMMoV and population is not as  
576 stable over time as caffeine and paraxanthine. In addition, our previous study confirmed that  
577 direct normalization effects of SARS-CoV-2 concentration using biomarker concentrations were  
578 always less ideal than indirect normalization, which involved the wastewater volume.<sup>29</sup>

579 Our findings suggest that for long-term wastewater SARS-CoV-2 surveillance, normalizing  
580 SARS-CoV-2 wastewater concentrations with a reliable population marker prior to calculating  
581 trends is highly recommended to account for changes in wastewater dilution and differences in  
582 relative human waste input over time due to tourism, weekday commuters, temporary workers,

583 and pandemic lockdowns, etc. This approach is particularly critical for the sewershed with  
584 dynamic population changes, such as colleges, tourist towns, and metropolitan areas, where a  
585 large number of commuters who used to travel to cities daily transitioned to fully or partially  
586 remote workers after the pandemic. The relation between 1) size of the population, and 2)  
587 strength of the relationship between wastewater SARS-CoV-2 viral concentration and the  
588 COVID-19 clinical incidence rate was first demonstrated in this study. This would provide an  
589 excellent selection criterion for site selection, surveillance planning and data interpretation for  
590 the SARS-CoV-2 and even other wastewater-based epidemiology.

## 591 **5. CONCLUSIONS**

592 This study compared the effectiveness of three wastewater biomarkers for population  
593 normalization in the SARS-CoV-2 wastewater-based epidemiology with a large number of  
594 wastewater facilities across Missouri and long-term sampling over seven months. We found that  
595 PMMoV, one of the widely used population biomarkers for SARS-CoV-2 wastewater-based  
596 epidemiology, is not an ideal population biomarker since it reduced the strength of wastewater  
597 SARS-CoV-2 viral load and the COVID-19 incidence rate compared to the metadata population  
598 and without population normalization. Instead, paraxanthine, with many benefits, such as high  
599 stability, low exogenous sources than its precursor (caffeine), higher recovery rate, and low  
600 quantification variation, is very promising for predicting the real-time population and population  
601 normalization in the wastewater SARS-CoV-2 surveillance study, no matter the size of the  
602 population. The utility of this promising biomarkers was validated by data from ten different  
603 Wisconsin's WWTPs with gradients in population sizes. The estimated real-time population  
604 using this biomarker was directly compared against the population patterns with human  
605 movement mobility data. Of the three biomarkers, population normalization by paraxanthine  
606 significantly strengthened the relationship between wastewater SARS-CoV-2 viral load and  
607 COVID-19 incidence rate the most (40 out of 61 sewersheds). Our findings suggest that  
608 paraxanthine has the potential to be serve as real-time population biomarker in other scenarios  
609 beyond SARS-CoV-2 wastewater-based epidemiology and not limited within Missouri  
610 geographical boundary.

## 611 **6. ACKNOWLEDGEMENT**

612 The authors would like to thank the Missouri Department of Health and Senior Services  
613 (DHSS) for administrating the funding. We would like to express our gratitude to the Missouri  
614 Department of Natural Resources (DNR) for coordinating the sample collection. Research  
615 reported in this publication was supported by funding from the Centers for Disease Control and  
616 the National Institute on Drug Abuse of the National Institutes of Health under award number  
617 U01DA053893-01. We would also like to thank the Center for Agroforestry at the University of  
618 Missouri, USDA/ARS Dale Bumpers Small Farm Research Center under agreement number 58-  
619 6020-6-001 from the USDA Agricultural Research Service for supporting part of this research.  
620 The content is solely the responsibility of the authors and does not necessarily represent the  
621 official views of the National Institutes of Health, the Centers for Disease Control or USDA-  
622 ARS.

## 623 7. REFERENCE

- 624 1. Choi PM, Tucharke BJ, Donner E, et al. Wastewater-based epidemiology biomarkers: Past,  
625 present and future. *TrAC Trends in Analytical Chemistry*. 2018;105:453-469.  
626 doi:10.1016/j.trac.2018.06.004
- 627 2. Medema G, Heijnen L, Elsinga G, Italiaander R, Brouwer A. Presence of SARS-  
628 Coronavirus-2 RNA in Sewage and Correlation with Reported COVID-19 Prevalence in the  
629 Early Stage of the Epidemic in The Netherlands. *Environ Sci Technol Lett*. 2020;7(7):511-  
630 516. doi:10.1021/acs.estlett.0c00357
- 631 3. McMahan CS, Self S, Rennert L, et al. COVID-19 wastewater epidemiology: a model to  
632 estimate infected populations. *The Lancet Planetary Health*. 2021;5(12):e874-e881.  
633 doi:10.1016/S2542-5196(21)00230-8
- 634 4. Wu F, Zhang J, Xiao A, et al. SARS-CoV-2 Titers in Wastewater Are Higher than Expected  
635 from Clinically Confirmed Cases. 2020;5(4):9.
- 636 5. Kumar M, Jiang G, Kumar Thakur A, et al. Lead time of early warning by wastewater  
637 surveillance for COVID-19: Geographical variations and impacting factors. *Chemical*  
638 *Engineering Journal*. 2022;441:135936. doi:10.1016/j.cej.2022.135936
- 639 6. Kirby AE, Walters MS, Jennings WC, et al. Using Wastewater Surveillance Data to  
640 Support the COVID-19 Response — United States, 2020–2021. *MMWR Morb Mortal Wkly*  
641 *Rep*. 2021;70(36):1242-1244. doi:10.15585/mmwr.mm7036a2
- 642 7. Chan AY, Kim H, Bell ML. Higher incidence of novel coronavirus (COVID-19) cases in  
643 areas with combined sewer systems, heavy precipitation, and high percentages of  
644 impervious surfaces. *Science of The Total Environment*. 2022;820:153227.  
645 doi:10.1016/j.scitotenv.2022.153227
- 646 8. Gracia-Lor E, Castiglioni S, Bade R, et al. Measuring biomarkers in wastewater as a new  
647 source of epidemiological information: Current state and future perspectives. *Environment*  
648 *International*. 2017;99:131-150. doi:10.1016/j.envint.2016.12.016
- 649 9. Medema G, Been F, Heijnen L, Petterson S. Implementation of environmental surveillance  
650 for SARS-CoV-2 virus to support public health decisions: Opportunities and challenges.  
651 *Current Opinion in Environmental Science & Health*. 2020;17:49-71.  
652 doi:10.1016/j.coesh.2020.09.006
- 653 10. Daughton CG. Real-time estimation of small-area populations with human biomarkers in  
654 sewage. *Science of The Total Environment*. 2012;414:6-21.  
655 doi:10.1016/j.scitotenv.2011.11.015
- 656 11. Chen C, Kostakis C, Gerber JP, Tucharke BJ, Irvine RJ, White JM. Towards finding a  
657 population biomarker for wastewater epidemiology studies. *Science of The Total*  
658 *Environment*. 2014;487:621-628. doi:10.1016/j.scitotenv.2013.11.075

- 659 12. McCall AK, Bade R, Kinyua J, et al. Critical review on the stability of illicit drugs in  
660 sewers and wastewater samples. *Water Research*. 2016;88:933-947.  
661 doi:10.1016/j.watres.2015.10.040
- 662 13. Been F, Rossi L, Ort C, Rudaz S, Delémont O, Esseiva P. Population Normalization with  
663 Ammonium in Wastewater-Based Epidemiology: Application to Illicit Drug Monitoring.  
664 *Environ Sci Technol*. 2014;48(14):8162-8169. doi:10.1021/es5008388
- 665 14. Sweetapple C, Wade MJ, Grimsley JMS, Bunce JT, Melville-Shreeve P, Chen AS.  
666 *Population Normalisation in Wastewater-Based Epidemiology for Improved Understanding*  
667 *of SARS-CoV-2 Prevalence: A Multi-Site Study*. *Epidemiology*; 2021.  
668 doi:10.1101/2021.08.03.21261365
- 669 15. Udert KM, Larsen TA, Gujer W. Fate of major compounds in source-separated urine. *Water*  
670 *Science and Technology*. 2006;54(11-12):413-420. doi:10.2166/wst.2006.921
- 671 16. van Nuijs ALN, Mougel JF, Tarcomnicu I, et al. Sewage epidemiology — A real-time  
672 approach to estimate the consumption of illicit drugs in Brussels, Belgium. *Environment*  
673 *International*. 2011;37(3):612-621. doi:10.1016/j.envint.2010.12.006
- 674 17. Holm RH, Nagarkar M, Yeager RA, et al. Surveillance of RNase P, PMMoV, and  
675 CrAssphage in wastewater as indicators of human fecal concentration across urban sewer  
676 neighborhoods, Kentucky. *FEMS Microbes*. 2022;3:xtac003. doi:10.1093/femsmc/xtac003
- 677 18. D'Aoust PM, Mercier E, Montpetit D, et al. Quantitative analysis of SARS-CoV-2 RNA  
678 from wastewater solids in communities with low COVID-19 incidence and prevalence.  
679 *Water Research*. 2021;188:116560. doi:10.1016/j.watres.2020.116560
- 680 19. Gasser G, Rona M, Voloshenko A, et al. Quantitative Evaluation of Tracers for  
681 Quantification of Wastewater Contamination of Potable Water Sources. *Environ Sci*  
682 *Technol*. 2010;44(10):3919-3925. doi:10.1021/es100604c
- 683 20. Oppenheimer J, Eaton A, Badruzzaman M, Haghani AW, Jacangelo JG. Occurrence and  
684 suitability of sucralose as an indicator compound of wastewater loading to surface waters in  
685 urbanized regions. *Water Research*. 2011;45(13):4019-4027.  
686 doi:10.1016/j.watres.2011.05.014
- 687 21. Kitajima M, Iker BC, Pepper IL, Gerba CP. Relative abundance and treatment reduction of  
688 viruses during wastewater treatment processes — Identification of potential viral indicators.  
689 *Science of The Total Environment*. 2014;488-489:290-296.  
690 doi:10.1016/j.scitotenv.2014.04.087
- 691 22. Kitajima M, Sassi HP, Torrey JR. Pepper mild mottle virus as a water quality indicator. *npj*  
692 *Clean Water*. 2018;1(1):19. doi:10.1038/s41545-018-0019-5
- 693 23. Daughton CG. Using biomarkers in sewage to monitor community-wide human health:  
694 Isoprostanes as conceptual prototype. *Science of The Total Environment*. 2012;424:16-38.  
695 doi:10.1016/j.scitotenv.2012.02.038



- 696 24. Thai PK, O'Brien JW, Banks APW, et al. Evaluating the in-sewer stability of three  
697 potential population biomarkers for application in wastewater-based epidemiology. *Science*  
698 *of The Total Environment*. 2019;671:248-253. doi:10.1016/j.scitotenv.2019.03.231
- 699 25. Heckman MA, Weil J, de Mejia EG. Caffeine (1, 3, 7-trimethylxanthine) in Foods: A  
700 Comprehensive Review on Consumption, Functionality, Safety, and Regulatory Matters.  
701 *Journal of Food Science*. 2010;75(3):R77-R87. doi:10.1111/j.1750-3841.2010.01561.x
- 702 26. Crews HM, Olivier L, Wilson LA. Urinary biomarkers for assessing dietary exposure to  
703 caffeine. *Food Addit Contam*. 2001;18(12):1075-1087. doi:10.1080/02652030110056630
- 704 27. Martínez Bueno MJ, Uclés S, Hernando MD, Dávoli E, Fernández-Alba AR. Evaluation of  
705 selected ubiquitous contaminants in the aquatic environment and their transformation  
706 products. A pilot study of their removal from a sewage treatment plant. *Water Research*.  
707 2011;45(6):2331-2341. doi:10.1016/j.watres.2011.01.011
- 708 28. Senta I, Gracia-Lor E, Borsotti A, Zuccato E, Castiglioni S. Wastewater analysis to monitor  
709 use of caffeine and nicotine and evaluation of their metabolites as biomarkers for  
710 population size assessment. *Water Research*. 2015;74:23-33.  
711 doi:10.1016/j.watres.2015.02.002
- 712 29. Hsu SY, Bayati MB, Li C, et al. *Biomarkers Selection for Population Normalization in*  
713 *SARS-CoV-2 Wastewater-Based Epidemiology*. *Epidemiology*; 2022.  
714 doi:10.1101/2022.03.14.22272359
- 715 30. U.S. Census. Population Density in Missouri Counties: 2020. Published 2020.  
716 <https://public.tableau.com/shared/CBTDRF3S8?:showVizHome=no>
- 717 31. Apple Maps. *COVID-19 Apple Mobility Trends Reports*.  
718 <https://aws.amazon.com/marketplace/pp/prodview-ucdg4nudicxzi#offers>
- 719 32. Robinson CA, Hsieh HY, Hsu SY, et al. Defining biological and biophysical properties of  
720 SARS-CoV-2 genetic material in wastewater. *Science of The Total Environment*.  
721 2022;807:150786. doi:10.1016/j.scitotenv.2021.150786
- 722 33. R Core Team. *R: A Language and Environment for Statistical Computing*. R Foundation for  
723 Statistical Computing; 2021. <https://www.R-project.org/>.
- 724 34. Ahmed W, Bivins A, Metcalfe S, et al. Evaluation of process limit of detection and  
725 quantification variation of SARS-CoV-2 RT-qPCR and RT-dPCR assays for wastewater  
726 surveillance. *Water Research*. 2022;213:118132. doi:10.1016/j.watres.2022.118132
- 727 35. Duvallet C, Wu F, McElroy KA, et al. Nationwide Trends in COVID-19 Cases and SARS-  
728 CoV-2 RNA Wastewater Concentrations in the United States. *ACS EST Water*. Published  
729 online May 3, 2022;acsestwater.1c00434. doi:10.1021/acsestwater.1c00434
- 730 36. Feng S, Roguet A, McClary-Gutierrez JS, et al. Evaluation of Sampling, Analysis, and  
731 Normalization Methods for SARS-CoV-2 Concentrations in Wastewater to Assess COVID-

- 732 19 Burdens in Wisconsin Communities. *ACS EST Water*. 2021;1(8):1955-1965.  
733 doi:10.1021/acsestwater.1c00160
- 734 37. Zhan Q, Babler KM, Sharkey ME, et al. Relationships between SARS-CoV-2 in  
735 Wastewater and COVID-19 Clinical Cases and Hospitalizations, with and without  
736 Normalization against Indicators of Human Waste. *ACS EST Water*. Published online May  
737 26, 2022:acsestwater.2c00045. doi:10.1021/acsestwater.2c00045
- 738 38. Rachmadi AT, Kitajima M, Pepper IL, Gerba CP. Enteric and indicator virus removal by  
739 surface flow wetlands. *Science of The Total Environment*. 2016;542:976-982.  
740 doi:10.1016/j.scitotenv.2015.11.001
- 741 39. Buerge IJ, Poiger T, Müller MD, Buser HR. Caffeine, an Anthropogenic Marker for  
742 Wastewater Contamination of Surface Waters. *Environ Sci Technol*. 2003;37(4):691-700.  
743 doi:10.1021/es020125z
- 744 40. Gracia-Lor E, Rousis NI, Zuccato E, et al. Estimation of caffeine intake from analysis of  
745 caffeine metabolites in wastewater. *Science of The Total Environment*. 2017;609:1582-  
746 1588. doi:10.1016/j.scitotenv.2017.07.258
- 747 41. Senchina DS, Hallam JE, Kohut ML, Nguyen NA. Alkaloids and athlete immune function:  
748 Caffeine, theophylline, gingerol, ephedrine, and their congeners. Published online 2014:26.
- 749 42. Colson P, Richet H, Desnues C, et al. Pepper Mild Mottle Virus, a Plant Virus Associated  
750 with Specific Immune Responses, Fever, Abdominal Pains, and Pruritus in Humans.  
751 Mylonakis E, ed. *PLoS ONE*. 2010;5(4):e10041. doi:10.1371/journal.pone.0010041
- 752 43. Haramoto E, Kitajima M, Kishida N, et al. Occurrence of Pepper Mild Mottle Virus in  
753 Drinking Water Sources in Japan. *Appl Environ Microbiol*. 2013;79(23):7413-7418.  
754 doi:10.1128/AEM.02354-13
- 755 44. Rosario K, Symonds EM, Sinigalliano C, Stewart J, Breitbart M. *Pepper Mild Mottle Virus*  
756 as an Indicator of Fecal Pollution. *Appl Environ Microbiol*. 2009;75(22):7261-7267.  
757 doi:10.1128/AEM.00410-09
- 758 45. Kato R, Asami T, Utagawa E, Furumai H, Katayama H. Pepper mild mottle virus as a  
759 process indicator at drinking water treatment plants employing coagulation-sedimentation,  
760 rapid sand filtration, ozonation, and biological activated carbon treatments in Japan. *Water*  
761 *Research*. 2018;132:61-70. doi:10.1016/j.watres.2017.12.068
- 762 46. Symonds EM, Sinigalliano C, Gidley M, Ahmed W, McQuaig-Ulrich SM, Breitbart M.  
763 Faecal pollution along the southeastern coast of Florida and insight into the use of pepper  
764 mild mottle virus as an indicator. *J of Applied Microbiology*. 2016;121(5):1469-1481.  
765 doi:10.1111/jam.13252
- 766 47. Olesen S. Interpreting building-level Covid-19 wastewater monitoring data. Published  
767 online 2021:13.

- 768 48. Bayati M, Hsieh HY, Hsu SY, et al. *Identification and Quantification of Bioactive*  
769 *Compounds Suppressing SARS-CoV-2 Signals in Wastewater-Based Epidemiology*  
770 *Surveillance*. *Epidemiology*; 2022. doi:10.1101/2022.03.09.22272155
- 771 49. Isaksson F, Lundy L, Hedström A, Székely AJ, Mohamed N. Evaluating the Use of  
772 Alternative Normalization Approaches on SARS-CoV-2 Concentrations in Wastewater:  
773 Experiences from Two Catchments in Northern Sweden. *Environments*. 2022;9(3):39.  
774 doi:10.3390/environments9030039
- 775

776 **Table 1.** Summary of the optimized LC-MSMS Parameters for chemical population biomarkers.

<b>No.</b>	<b>Compound</b>	<b>RT</b>	<b>ES</b>	<b>MS1</b>	<b>MS2</b>	<b>Cone Voltage</b>	<b>Collision Energy</b>
1	Caffeine	6.273	ES+	195.05	138.12	45	22
2	Caffeine- <sup>13</sup> C <sub>3</sub>	6.167	ES+	198.04	140.07	45	22
3	Paraxanthine	5.715	ES+	181.06	124.11	45	22

777

778 Table 2. Summary of ratios between estimated real-time population by three biomarkers to the  
779 Metadata population.

<b>Ratios</b>	<b>Mean</b>	<b>Max</b>	<b>Min</b>	<b>SD</b>
Caffeine-population/metadata population	1.248	79.669	0.008	1.862
Paraxanthine-population/metadata population	1.137	12.053	0.008	0.741
PMMoV-population/metadata population	1.471	75.203	0.00008	2.26

780



781 **Table 3.** Coefficient of determinations ( $R^2$ ) of the linear regression models between log-  
 782 transformed wastewater SARS-CoV-2 RNA load (copies/week/10K person) and clinical  
 783 COVID-19 incidence rate (case number/week/10K person) within each WWTP without and with  
 784 population normalization by metadata population, and the real-time populations estimated from  
 785 caffeine, paraxanthine, and PMMoV. The bold and underlined values are the highest  $R^2$  for each  
 786 WWTP among five models. “N.S.” indicates the not significant models. “N.A. indicated not  
 787 available information.

Facility ID	Popula tion Served	Total cases	Without population normalizatio n	Metadata population normalization	Caffeine estimated real-time population normalizatio n	Paraxanthine estimated real-time population normalizatio n	PMMoV estimated real-time population normalizatio n
ANON1	900	13	0.229	0.223	0.220	<b><u>0.257</u></b>	N.S.
ALBNY	1730	178	0.781	0.802	0.799	<b><u>0.827</u></b>	0.786
MEMPH	1822	24	0.206	0.197	0.214	<b><u>0.232</u></b>	0.196
MILAN	1960	83	0.470	<b><u>0.478</u></b>	0.401	0.473	0.287
WLOSP	2100	82	N.S.	N.S.	N.S.	N.S.	N.S.
TRYSE	2934	1015	0.761	0.683	0.569	<b><u>0.763</u></b>	0.741
WARSW	2976	127	0.136	0.160	0.215	<b><u>0.254</u></b>	0.242
CASVL	3300	155	0.399	0.368	0.337	<b><u>0.406</u></b>	0.280
CAROL	3784	285	0.539	0.542	0.593	<b><u>0.644</u></b>	0.561
CHARL	4000	102	N.S.	N.S.	N.S.	N.S.	N.S.
BROOK	4600	84	0.375	0.369	0.338	0.405	<b><u>0.556</u></b>
ELDON	4895	312	0.481	<b><u>0.496</u></b>	0.359	0.485	0.246
MACON	5471	95	0.297	0.309	0.351	<b><u>0.452</u></b>	N.S.
DEXTW	6000	211	0.620	<b><u>0.634</u></b>	0.467	0.576	0.340
ANON2	6155	429	0.462	<b><u>0.470</u></b>	0.420	0.445	0.136
PACIF	7001	260	0.675	0.676	0.603	0.685	<b><u>0.745</u></b>
SDLCN	7500	218	<b><u>0.728</u></b>	0.725	0.390	0.576	0.283
UNONW	7936	1208	0.738	0.740	0.764	<b><u>0.765</u></b>	0.697
MARSH	8000	539	0.505	0.503	0.471	<b><u>0.563</u></b>	0.524
NEVAD	8082	955	0.332	0.328	0.287	<b><u>0.376</u></b>	0.468
SDLNO	8250	80	N.S.	N.S.	N.S.	N.S.	N.S.
PRYVL	9000	645	0.391	0.393	0.328	<b><u>0.417</u></b>	0.322
KCTDC	9000	618	0.827	0.828	0.813	<b><u>0.851</u></b>	0.749
MONET	9100	338	0.693	0.693	0.687	<b><u>0.761</u></b>	0.634
MRSHL	10113	716	0.407	0.407	<b><u>0.567</u></b>	0.526	0.564
FRMTN	10114	775	0.590	0.590	0.544	<b><u>0.649</u></b>	0.549
BLIVR	10500	466	0.611	0.610	0.614	<b><u>0.645</u></b>	0.643
ANON3	10559	378	0.350	0.352	0.303	<b><u>0.417</u></b>	0.251
SDLSE	10730	225	0.7657	<b><u>0.7659</u></b>	0.464	0.697	0.306
MEXCO	11500	752	0.703	0.697	0.667	<b><u>0.707</u></b>	0.548
WARNE	11883	574	0.560	0.558	0.530	0.605	<b><u>0.832</u></b>
CARTH	12000	606	0.593	0.596	0.490	<b><u>0.646</u></b>	0.422
ANON4	12000	642	0.766	0.771	0.743	<b><u>0.791</u></b>	0.581
WPLAN	12000	726	0.879	0.882	0.882	0.893	<b><u>0.940</u></b>
KCROB	12000	665	0.610	0.616	0.591	<b><u>0.646</u></b>	0.410
KCFSR	12000	525	0.588	0.590	0.575	0.578	<b><u>0.639</u></b>
FULTN	12790	859	0.358	0.363	0.333	<b><u>0.402</u></b>	0.300
WARNW	14477	389	0.659	0.653	0.701	<b><u>0.721</u></b>	0.666
WASHN	15000	691	<b><u>0.659</u></b>	0.655	0.524	0.657	0.570
JOPSC	15906	426	0.729	0.733	0.737	<b><u>0.795</u></b>	0.675
HANBL	16000	727	0.414	0.416	0.490	<b><u>0.512</u></b>	0.307
SKSTN	17000	1289	0.674	0.680	<b><u>0.685</u></b>	0.677	0.570
NIXAF	20000	1118	0.680	0.678	0.669	<b><u>0.698</u></b>	0.693
SFDNW	22818	2826	0.731	0.727	0.715	0.733	<b><u>0.771</u></b>
MSDFN	24174	1633	0.515	0.527	0.435	<b><u>0.543</u></b>	0.376

It is made available under a [CC-BY-ND 4.0 International license](https://creativecommons.org/licenses/by-nd/4.0/) .

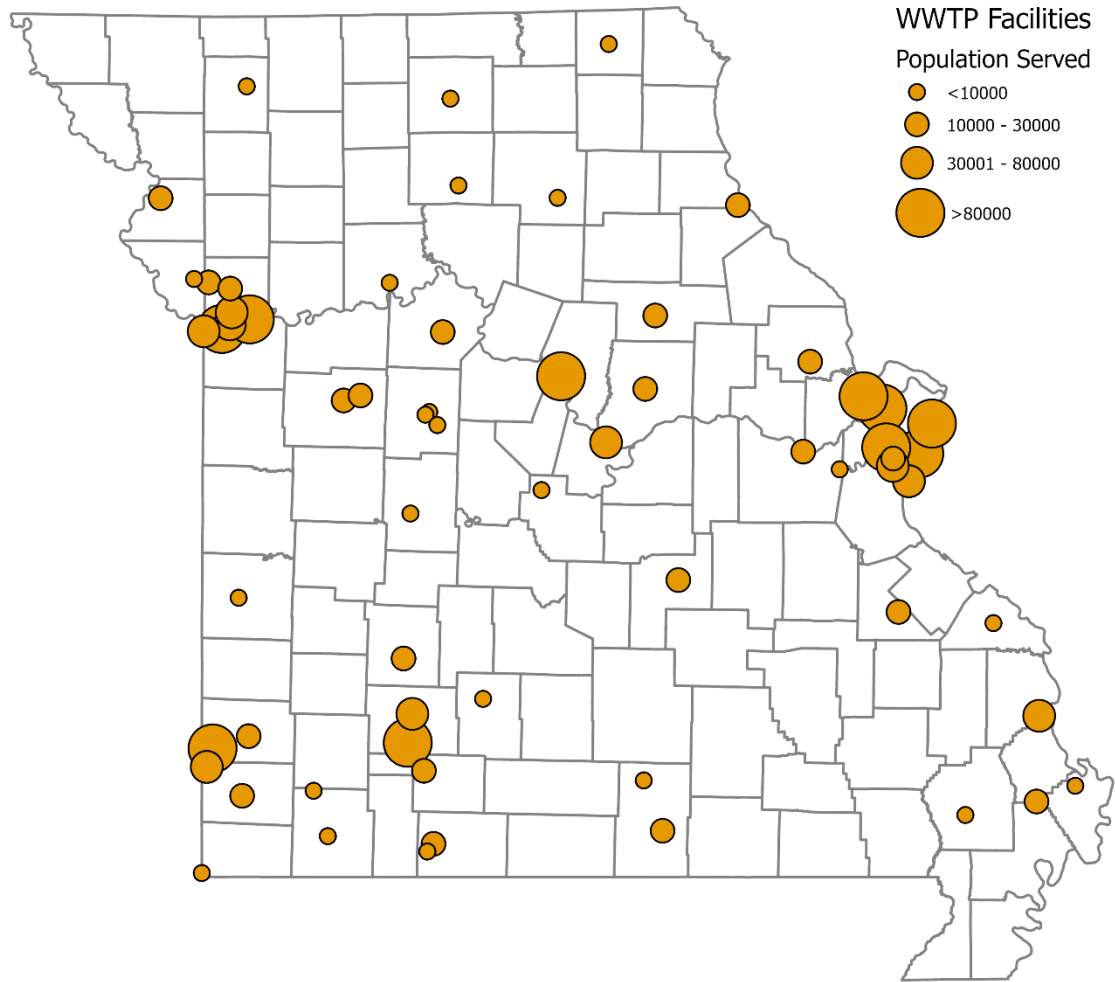
<b>ROLSE</b>	25423	1309	0.676	<b><u>0.681</u></b>	0.545	0.668	0.475
<b>STJOE</b>	27000	5048	0.787	0.787	0.740	<b><u>0.851</u></b>	0.533
<b>NPSDS</b>	27391	1841	0.657	0.656	0.613	<b><u>0.705</u></b>	0.487
<b>CAPEG</b>	33540	1653	0.591	0.599	0.474	<b><u>0.698</u></b>	0.401
<b>JOPTC</b>	34403	2176	<b><u>0.872</u></b>	0.861	0.852	0.871	0.766
<b>LIBTY</b>	35300	1534	0.8537	0.853	0.811	<b><u>0.8541</u></b>	0.749
<b>JEFFC</b>	41153	2861	0.759	0.766	0.776	<b><u>0.806</u></b>	0.645
<b>STPSC</b>	60000	3998	0.792	0.780	0.770	<b><u>0.809</u></b>	0.800
<b>KCWST</b>	61250	1926	0.826	0.814	0.798	<b><u>0.840</u></b>	0.792
<b>MSDLM</b>	66738	3677	0.789	0.790	0.726	<b><u>0.795</u></b>	0.728
<b>KCBIR</b>	76759	4455	<b><u>0.904</u></b>	0.902	0.777	0.883	0.798
<b>MSDGG</b>	115895	7392	0.797	0.787	0.764	<b><u>0.809</u></b>	0.664
<b>COLMB</b>	123180	6607	0.783	0.763	0.741	<b><u>0.810</u></b>	0.640
<b>SFDSW</b>	151966	8465	0.866	0.842	0.822	0.899	<b><u>0.905</u></b>
<b>MSDMR</b>	174537	11632	0.854	0.859	0.844	<b><u>0.864</u></b>	0.799
<b>MSDBP</b>	306647	15950	0.662	0.663	0.681	<b><u>0.756</u></b>	0.562
<b>LBVAT</b>	360000	16524	0.938	0.930	0.932	<b><u>0.944</u></b>	0.899
<b>MSDME</b>	451367	22557	0.874	0.872	<b><u>0.906</u></b>	0.888	0.723
<b>KCBLU</b>	N.A.	8020	0.638	N.A.	0.510	<b><u>0.645</u></b>	0.409

788

789 Table 4. Case study in the smallest WWTP ANON1 (900 population) for the process limit of  
 790 detection of wastewater SARS-CoV-2 surveillance. The process limit of detection (PLOD) of  
 791 N1N2 mass load PLOD1 for at least one case was calculated based on the results of this study  
 792 (Figure 7B). The PLOD2 was calculated based on the literature.<sup>34</sup> The bold and underling values  
 793 were the three weeks that N1N2 mass load higher both PLOD1 and PLOD2.

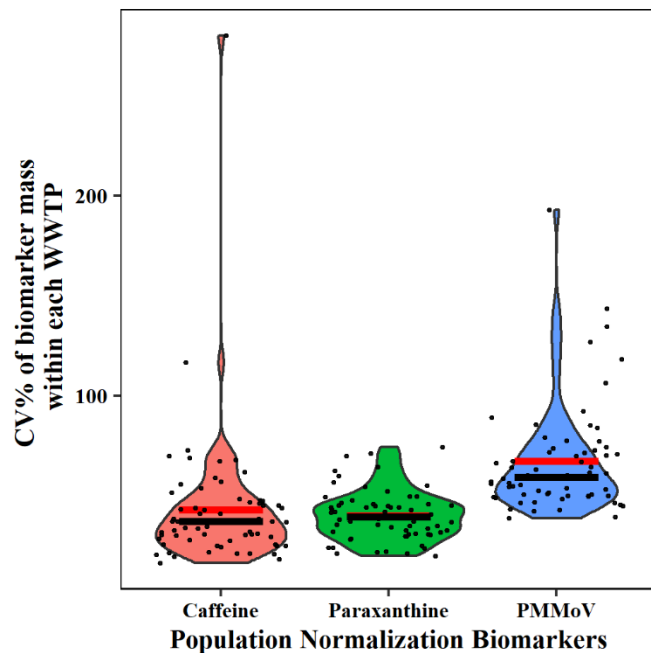
SWCTY Cases	Flow rate (GMD)	Week	N1N2 mass load	N1N2 mass - PLOD1	N1N2 mass - PLOD2
0	0.0425	9/13/2021	5.56E+10	-7.44E+10	-3.35E+10
0	0.0639	9/20/2021	7.10E+10	-5.90E+10	-6.29E+10
0	0.0535	9/27/2021	9.22E+10	-3.78E+10	-1.99E+10
1	0.0531	10/04/2021	7.85E+10	-5.15E+10	-3.28E+10
0	0.0553	10/11/2021	1.62E+10	-1.14E+11	-9.97E+10
0	0.0488	10/18/2021	4.92E+10	-8.08E+10	-5.31E+10
0	0.0562	10/25/2021	1.38E+10	-1.16E+11	-1.04E+11
0	0.0546	11/8/2021	6.63E+09	-1.23E+11	-1.08E+11
0	0.0512	11/15/2021	1.45E+10	-1.16E+11	-9.28E+10
0	0.0474	11/22/2021	8.18E+10	-4.82E+10	-1.75E+10
1	0.0458	11/29/2021	7.91E+10	-5.09E+10	-1.69E+10
0	0.0493	12/6/2021	1.54E+10	-1.15E+11	-8.79E+10
2	0.053	12/13/2021	4.32E+09	-1.26E+11	-1.07E+11
<b>1</b>	<b>0.0544</b>	<b>12/20/2021</b>	<b>7.34E+11</b>	<b>6.04E+11</b>	<b>6.20E+11</b>
<b>6</b>	<b>0.0544</b>	<b>1/10/2022</b>	<b>1.98E+12</b>	<b>1.85E+12</b>	<b>1.87E+12</b>
0	0.0573	1/31/2022	6.01E+10	-6.99E+10	-6.00E+10
<b>0</b>	<b>0.06</b>	<b>2/7/2022</b>	<b>1.37E+11</b>	<b>7.00E+09</b>	<b>1.13E+10</b>
2	0.06	2/14/2022	9.48E+10	-3.52E+10	-3.09E+10
0	0.0608	2/21/2022	4.69E+09	-1.25E+11	-1.23E+11
0	0.06	2/28/2022	3.36E+08	-1.30E+11	-1.25E+11
0	0.072	3/7/2022	1.44E+09	-1.29E+11	-1.49E+11
0	0.07	3/14/2022	9.97E+08	-1.29E+11	-1.46E+11
0	0.11	3/21/2022	2.18E+09	-1.28E+11	-2.28E+11
0	0.05	3/28/2022	6.19E+08	-1.29E+11	-1.04E+11

794



795

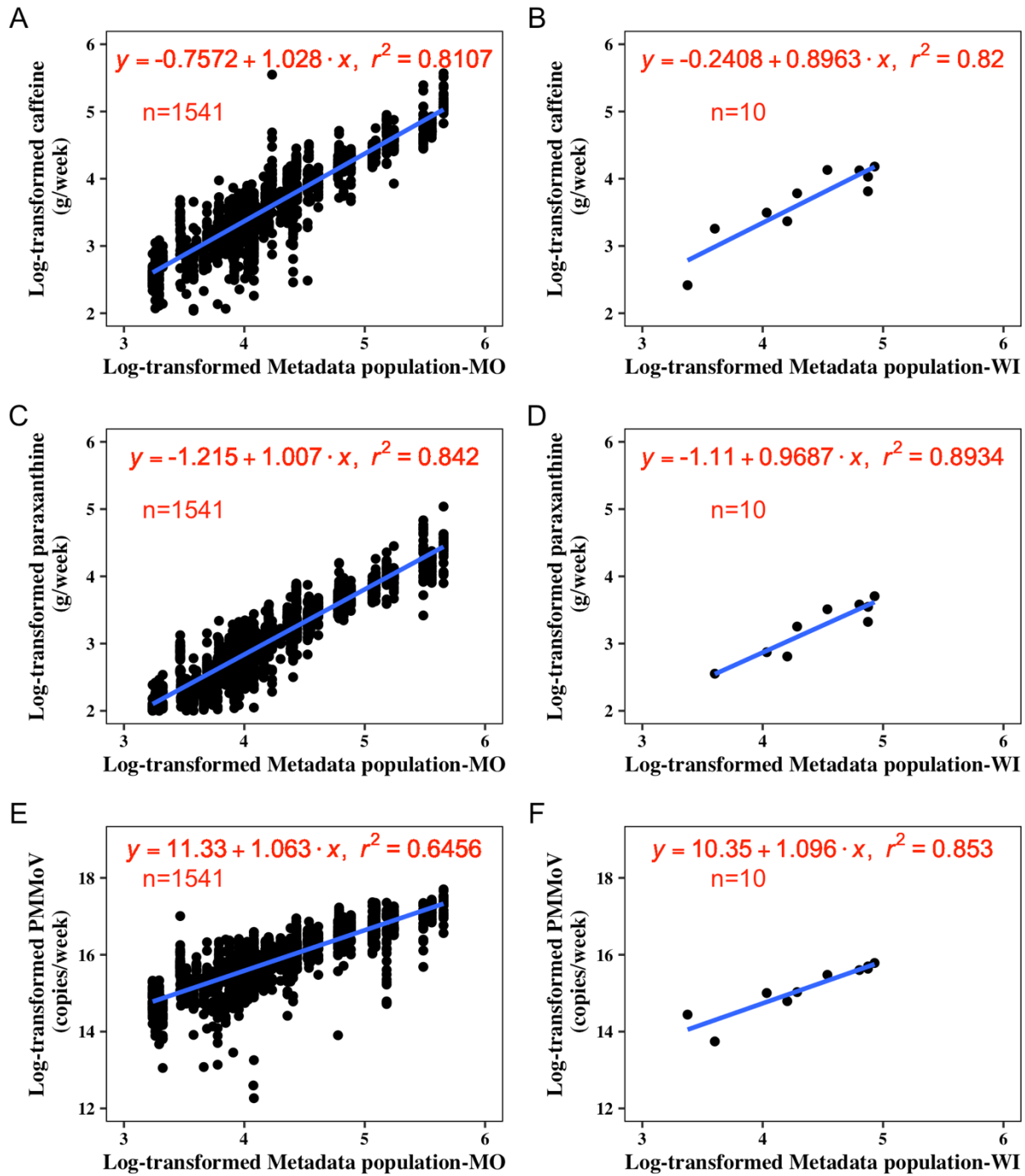
796 **Fig. 1.** A total of 2624 wastewater samples were collected from 64 wastewater treatment plants  
797 (WWTPs) across Missouri, USA.



798

799 **Fig. 2.** Distributions of coefficient of variation (CV%) of three biomarkers over seven months of  
800 study time from 09/13/2021 to 04/10/2022 (n=1569) within 64 WWTPs. The red lines indicate  
801 the mean CV%, and the black lines indicate the median CV% of each biomarker.

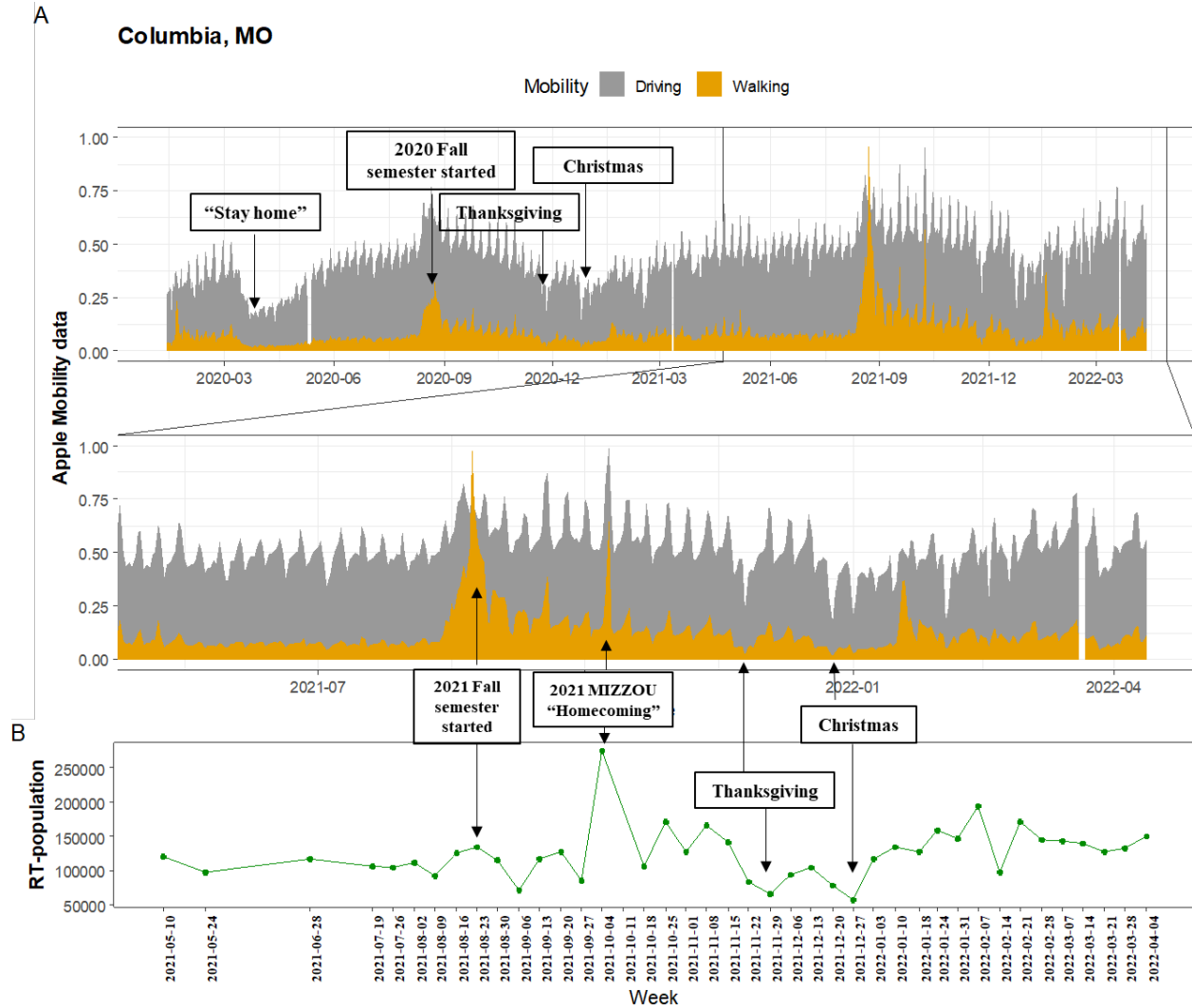




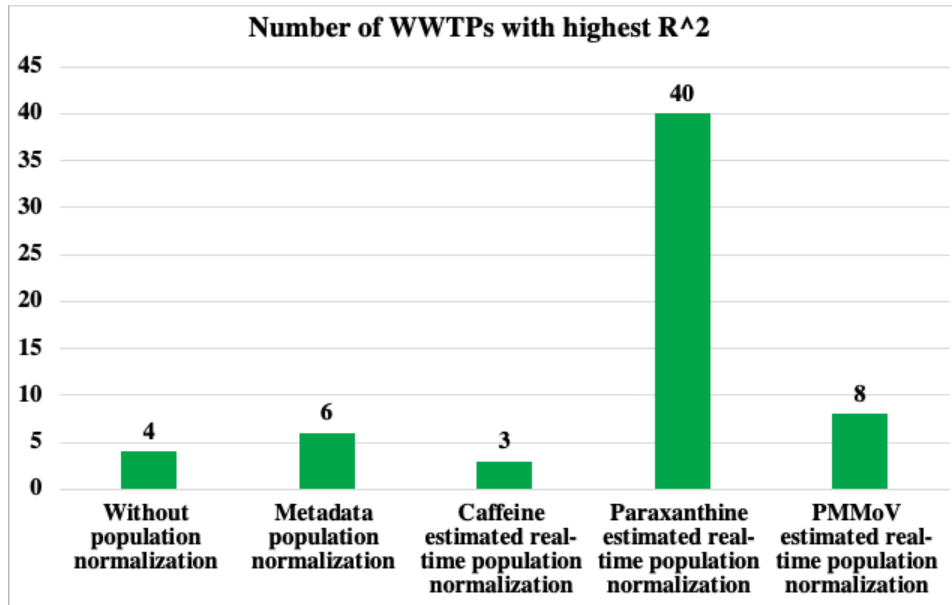
802

803 Fig. 3. The linear regression models between the mass loads of three wastewater biomarkers  
804 [(caffeine, paraxanthine, and pepper mild mottle virus (PMMoV))] and Metadata population  
805 (GIS-mapped census population or estimated from sewer connections) for Missouri based on 7-  
806 month wastewater samples collected from 09/13/21 to 04/10/22 across 63 wastewater treatment  
807 plants (WWTPs) (plot A, C, and E). One facility from the initial 64 WWTPs (WWTP KCBLU)  
808 was removed from the models since the population served changed dramatically during the

809 sampling period due to facility upgrading. Plots of B, D, and F were the models for Wisconsin  
810 based on ten samples collected during the week of 06/07/2021 from ten different WWTPs.



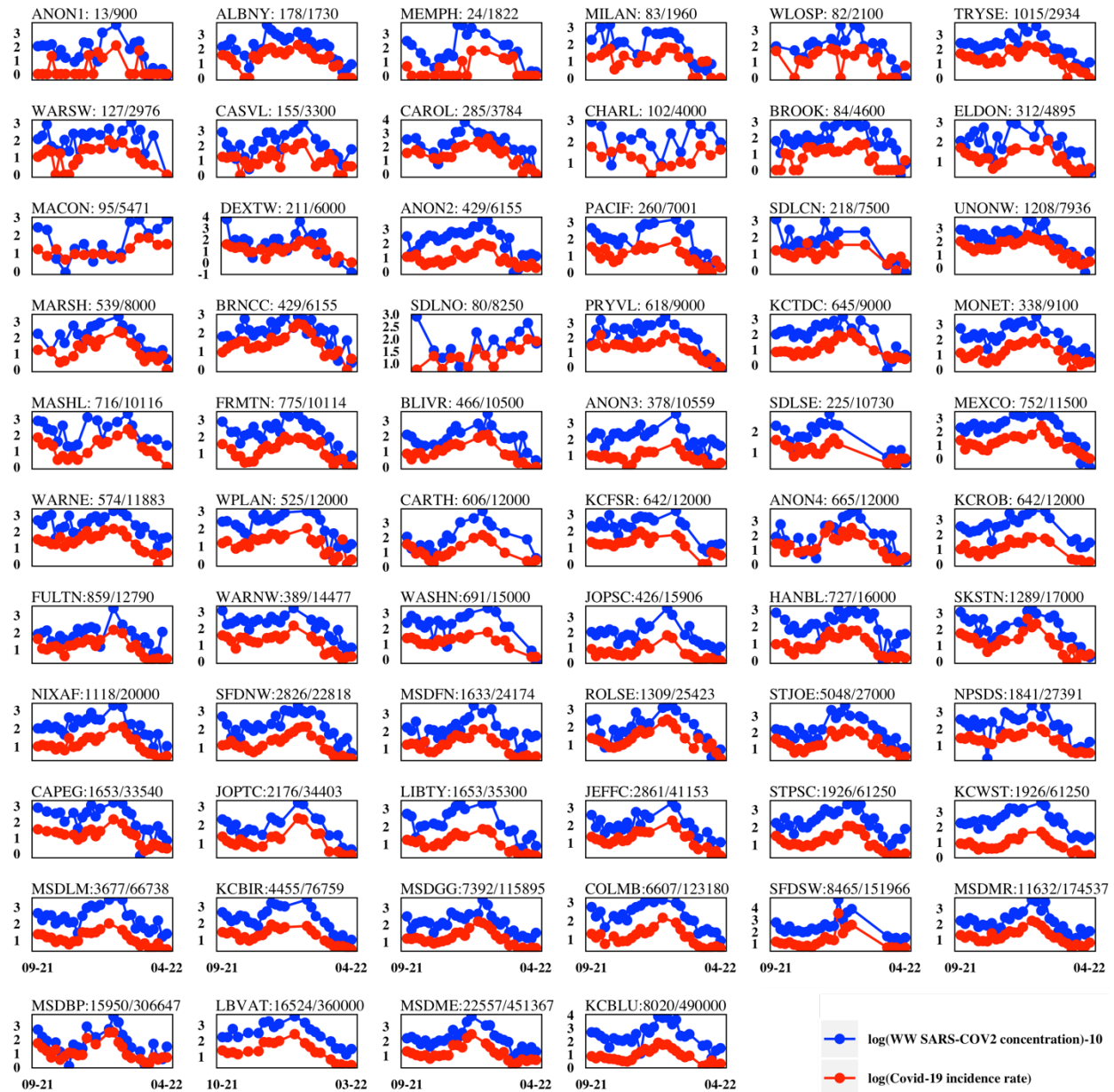
811  
812 Fig. 4. Apple mobility indices of Columbia, MO for walking and driving using aggregated data  
813 collected from Apple Maps data for the duration of 01/13/2020 to 04/10/2022 (A). The original  
814 Apple mobility indices have been scaled to the maximum observed during the study period.  
815 Predicted real-time population using paraxanthine in Columbia, MO (B).



816

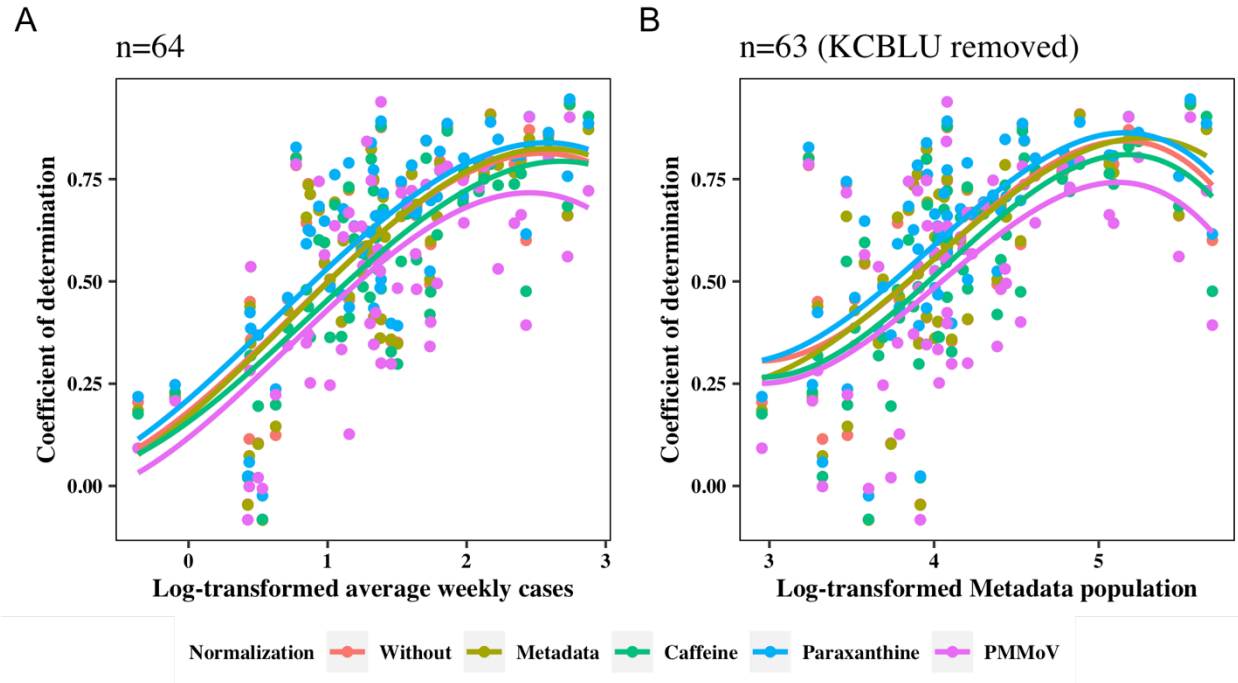
817 Fig. 5. The WWTP numbers with best population normalization models (highest  $R^2$ ) for each  
818 normalization model. The “61” after slash indicated the 61 out of 64 WWTPs had significant  
819 linear regression models between wastewater SARS-CoV-2 RNA load (copies/week/10K  
820 person) and clinical COVID-19 incidence rate (case/week/10K person). The numbers before the  
821 slash indicated the number of WWTPs with the highest  $R^2$  among the five regression models.

It is made available under a [CC-BY-ND 4.0 International license](https://creativecommons.org/licenses/by-nd/4.0/) .



822

823 Fig. 6. Normalized wastewater SARS-CoV-2 RNA load (copies/week/10K person) by  
 824 paraxanthine estimated real-time population and clinical COVID-19 incidence rate  
 825 (case/week/10K person) within 64 WWTPs from the weeks of 09/13/2021 to 04/05/2022. The  
 826 population of WWTPs increase from top left to right down. The title of each plot is in the format  
 827 of “WWTP name: total COVID-19 case number/Metadata population”.



828

829 Fig. 7. The polynomial relationships between the coefficient of determination ( $R^2$ ) of the linear  
830 regression models and clinical case (A) and Metadata population (B). The models were linear  
831 regressions between wastewater SARS-CoV-2 RNA load (copies/week/10K person) and clinic  
832 COVID-19 incidence rate (cases/week/10K person) within 64 WWTPs without and with the  
833 population normalizations.



834 **Table S1.** Long-time monitoring wastewater facilities across Missouri state and population sizes  
835 it served.

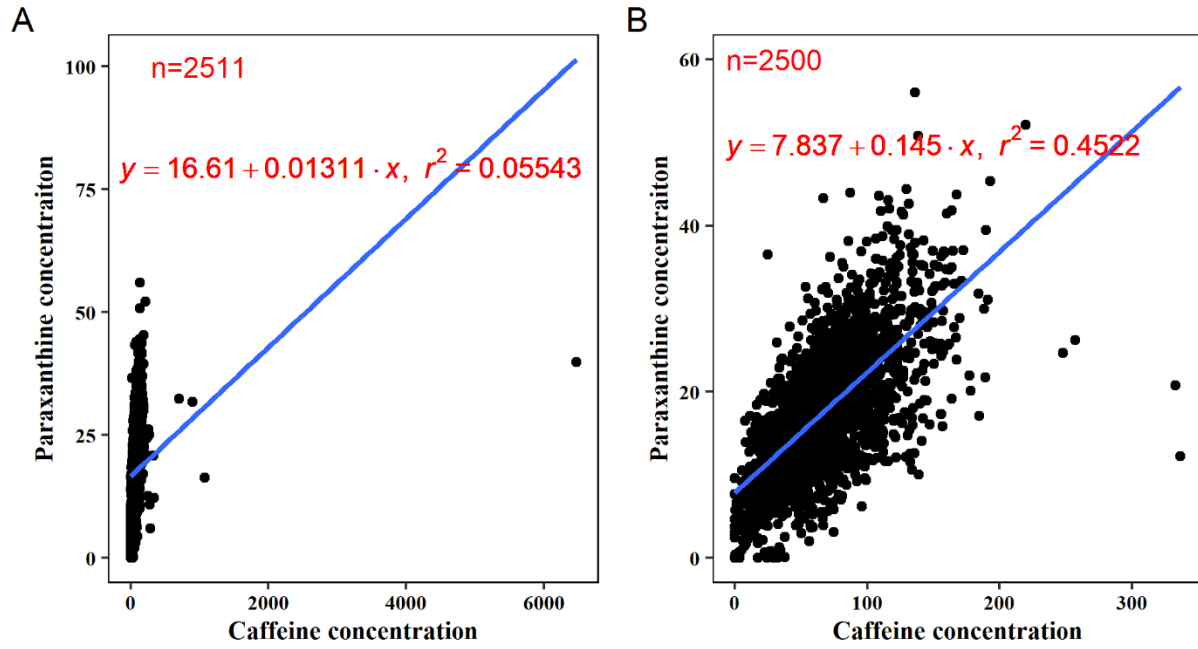
Facility ID	Facility Name	City	County	Population Served	Source of Population	Facility Capacity (MGD)	Composite sampling mode
ANON1	Anonymous WWTP#1			900	Operator information	0.14	Time Based
ALBNY	Albany WWTF	Albany	Gentry	1,730	Operator information	0.49	Time Based
MEMPH	Memphis Municipal WWTF	Memphis	Scotland	1,822	Operator information	0.21	Time Based
MILAN	Milan WWTP	Milan	Sullivan	1,960	Operator information	0.7	Flow Based
WLOSP	Willow Springs WWTP	Willow Springs	Howell	2,100	Operator information	0.4	Time Based
TRYSE	Troy Southeast WWTP	Troy	Lincoln	2,934	Connections w/ pop. Correction	0.45	Flow Based
WARSW	Warsaw WWTF	Warsaw	Benton	2,976	Operator information	1.1	Time Based
CASVL	Cassville WWTP	Cassville	Barry	3,300	Operator information	1.5	Time Based
CAROL	Carrollton WWTP	Carrollton	Carroll	3784	Operator information	1.5	Time Based
CHARL	Charleston	Charleston	Mississippi	4,000	Operator information	2	Time Based
BROOK	Brookfield WWTP	Brookfield	Linn	4,600	Operator information	1	Time Based
ELDON	Eldon WWTP	Eldon	Miller	4,895	Operator information	2.5	Time Based
MACON	Macon WWTP	Macon	Macon	5,471	Operator information	0.78	Time Based
DEXTW	Dexter West WWTP	Dexter	Stoddard	6,000	Operator information	3.4	Time Based
ANON2	Anonymous WWTP#2			6,155	Operator information	2	Time Based
PACIF	Pacific WWTP	Pacific	Franklin	7,001	Operator information	3.03	Time Based
SDLCN	Sedalia Central WWTP	Sedalia	Pettis	7,500	Connections w/ pop. Correction	1.5	Time Based
UNONW	Union West STP	Union	Franklin	7,936	Operator information	1.5	Time Based
MARSH	Marshfield WWTP	Marshfield	Webster	8,000	Connections w/ pop. Correction	2	Time Based
NEVAD	Nevada WWTF	Nevada	Vernon	8,082	Operator information	2.5	Time Based
SDLNO	Sedalia North WWTP	Sedalia	Pettis	8,250	Operator information	1.8	Time Based
PRYVL	Perryville SE WWTP	Perryville	Perry	9,000	Operator information	3.4	Time Based
KCTDC	KC, Todd Creek WWTP	Kansas City	Platte	9,000	Operator information	6	Time Based
MONET	Monett Wastewater Treatment Plant	Monett	Barry	9,100	Operator information	1	Time Based
MRSHL	Marshall SE WWTP	Marshall	Saline	10,113	Operator information	7.1	Time Based
FRMTN	Farmington East WWTP	Farmington	St. Francois	10,114	Operator information	2.55	Time Based
BLIVR	Bolivar WWTP	Bolivar	Polk	10,500	Operator information	5.3	Time Based
ANON3	Anonymous WWTP#3			10,559	Connections w/ pop. Correction	2.6	Time Based
SDLSE	Sedalia Southeast WWTP	Sedalia	Pettis	10,730	Operator information	3	Time Based
MEXCO	Mexico WWTP	Mexico	Audrain	11,500	Operator information	1.5	Flow Based
WARNE	Warrensburg East WWTP	Warrensburg	Johnson	11,883	Operator information	7	Time Based

It is made available under a [CC-BY-ND 4.0 International license](https://creativecommons.org/licenses/by-nd/4.0/) .

CARTH	Carthage WWTP	Carthage	Jasper	12,000	Operator information	9	Time Based
ANON4	Anonymous WWTP#4			12,000	Operator information	3	Time Based
WPLAN	West Plains WWTP	West Plains	Howell	12,000	Operator information	2.8	Time Based
KCROB	KC Rocky Branch WWTP	Kansas City	Clay	12,000	Operator information	2	Time Based
KCFSR	KC, Fishing River WWTF	Kansas City	Clay	12,000	Operator information	2.9	Time Based
FULTN	Fulton WWTP	Fulton	Callaway	12,790	Operator information	1.5	Flow Based
WARNW	Warrensburg West WWTP	Warrensburg	Johnson	14,477	Operator information	4.8	Time Based
WASHN	Washington WWTP	Washington	Franklin	15,000	Operator information	4	Time Based
JOPSC	Joplin Shoal Creek WWTP	Joplin	Newton	15,906	Connections w/ pop. Correction	7.2	Time Based
HANBL	Hannibal WWTP	Hannibal	Marion/Ralls	16,000	Operator information	12	Time Based
SKSTN	Sikeston WWTP	Sikeston	Scott	17,000	Operator information	2.75	Time Based
NIXAF	Nixa WWTF	Nixa	Christian	20,000	Operator information	5	Time Based
SFDNW	Springfield NW WWTP	Springfield	Greene	22,818	Operator information	4	Time Based
MSDFN	MSD Fenton WWTP	St. Louis	St. Louis	24,174	Connections w/ pop. Correction	6.8	Time Based
ROLSE	Rolla SE WWTP	Rolla	Phelps	25,423	Operator information	6.75	Time Based
STJOE	St. Joseph Water Protection Facility	St. Joseph	Buchanan	27,000	Connections w/ pop. Correction	27	Time Based
NPSDS	NPSD Interim Saline Creek Regional WWTP	FENTON	Jefferson	27,391	Connections w/ pop. Correction	4	Time Based
CAPEG	Cape Girardeau Municipal WWTF	Cape Girardeau	Cape Girardeau	33,540	Connections w/ pop. Correction	15	Time Based
JOPTC	Joplin Turkey Creek WWTP	Joplin	Jasper	34,403	Operator information	5	Time Based
LIBTY	Liberty WWTP	Liberty	Clay	35,300	Operator information	11	Flow Based
JEFFC	Jefferson City RWRf	Jefferson City	Callaway	41,153	Operator information	9.5	Time Based
STPSC	St. Peters Spencer Creek WWTP	St. Peters	St. Charles	60,000	Connections w/ pop. Correction	22.5	Time Based
KCWST	KC, Westside WWTP	Kansas City	Jackson	61,250	Operator information	15	Time Based
MSDLM	MSD Lower Meramec WWTP	St. Louis	St. Louis	66,738	Operator information	11	Flow Based
KCBIR	KC Birmingham WWTP	Kansas City	Clay	76,759	Connections w/ pop. Correction	20	Time Based
MSDGG	MSD Grand Glaize WWTP	Valley Park	St. Louis	115,895	Operator information	21	Time Based
COLMB	Columbia WWTP	Columbia	Boone	123,180	Operator information	20.6	Time Based
SFDSW	Springfield SW WWTP	Springfield	Greene	151,966	Connections w/ pop. Correction	64	Time Based
MSDMR	MSD Missouri River WWTP	St. Louis	St. Louis	174,537	Operator information	38	Time Based
MSDBP	MSD Bissell Point WWTP	St. Louis	St. Louis City	306,647	Operator information	150	Time Based
LBVAT	LBVSD Atherton WWTP	Independence	Jackson	360,000	Population Equivalent	52	Time Based
MSDME	MSD Lemay WWTP	St. Louis	St. Louis	451,367	Operator information	210	Time Based
KCBLU	KC Blue River WWTP	Kansas City	Jackson	490,000	Operator information	105	Time Based

837 **Table S2.** Comparison of caffeine and paraxanthine concentrations from two sample preparation  
 838 methods with samples of weeks of December 6, 2021. “M” indicated dilution solution was  
 839 methanol, and the corresponding sample above with the same sample I.D. and date (e.g., 1-12/7)  
 840 but without “M” means method with acidification and dilution solution was LC-MSMS buffer.

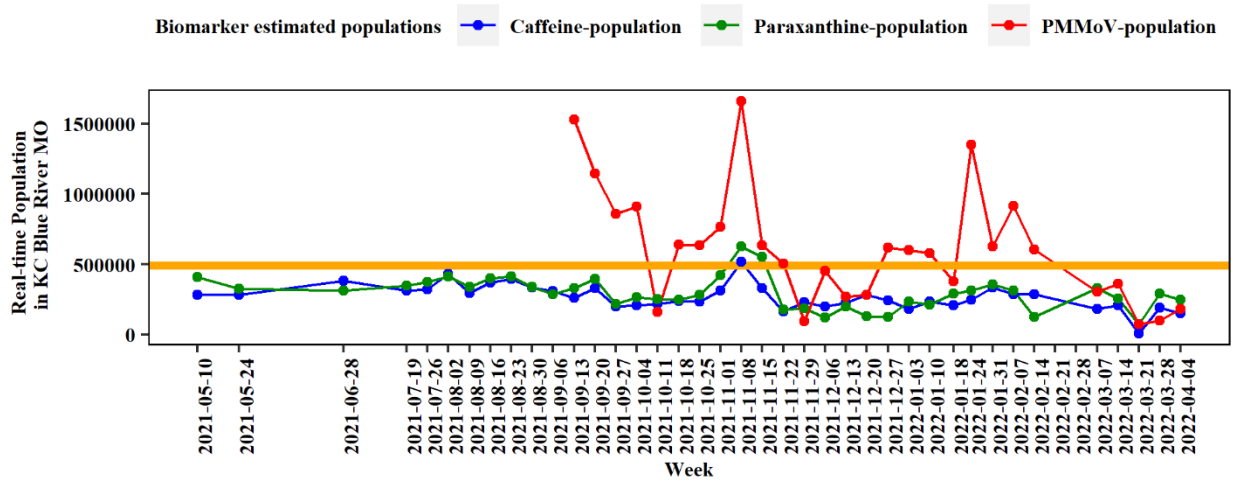
Samples lab I.D.	Caffeine concentration (ug/L)	Paraxanthine concentration (ug/L)
1-12/7	53.77	12.47
1-12/7M	54.37	9.54
2-12/6	130.57	20.00
2-12/6M	128.92	17.16
3-12/7	143.90	21.28
3-12/7M	158.40	22.45
4-12/7	59.64	9.66
4-12/7M	66.07	8.59
5-12/6	108.25	14.51
5-12/6M	111.08	14.71
6-12/7	42.41	8.79
6-12/7M	45.35	12.72
7-12/8	22.48	0.66
7-12/8M	24.50	0.92
9-12/6	65.94	7.71
9-12/6M	63.93	7.32
10-12/7	84.42	8.80
10-12/7M	84.41	9.60
11-12/6	60.38	16.19
11-12/6M	61.49	18.10
12-12/8	48.53	4.08
12-12/8M	47.14	5.51
14-12/7	115.88	25.76
14-12/7M	121.46	23.36
15-12/7	70.25	5.61
15-12/7M	77.87	6.26
16-12/7	122.98	22.27
16-12/7M	135.14	22.38
18-12/7	87.00	19.71
18-12/7M	98.78	24.42
19-12/7	78.86	15.28
19-12/7M	83.29	16.23
20-12/7	98.70	13.56
20-12/7M	105.32	13.75
22-12/6	101.51	15.80
22-12/6M	107.08	18.08
23-12/6	51.84	19.90
23-12/6M	57.01	14.51
24-12/6	27.90	8.05
24-12/6M	29.00	7.06
25-12/7	107.68	21.25
25-12/7M	112.49	25.92
26-12/7	78.37	14.44
26-12/7M	84.80	15.19
27-12/7	141.10	29.72
27-12/7M	146.91	28.84
28-12/7	64.87	7.87
28-12/7M	70.24	7.71
29-12/7	45.03	10.61
29-12/7M	48.56	12.92
30-12/8	74.65	11.97
30-12/8M	75.51	15.27
31-12/7	70.36	10.81
31-12/7M	79.95	10.13
34-12/6	86.26	13.51
34-12/6M	91.11	13.74
35-12/7	52.33	8.81
35-12/7M	60.88	9.27
36-12/7	58.39	5.94
36-12/7M	66.11	6.94
37-12/6	72.33	6.13
37-12/6M	71.84	7.06
38-12/7	1073.50	16.30
38-12/7M	1164.20	16.38
39-12/7	36.39	0.00
39-12/7M	39.24	0.00
41-12/8	71.57	10.40
41-12/8M	73.37	10.75
42-12/7	49.39	8.23
42-12/7M	56.02	8.50



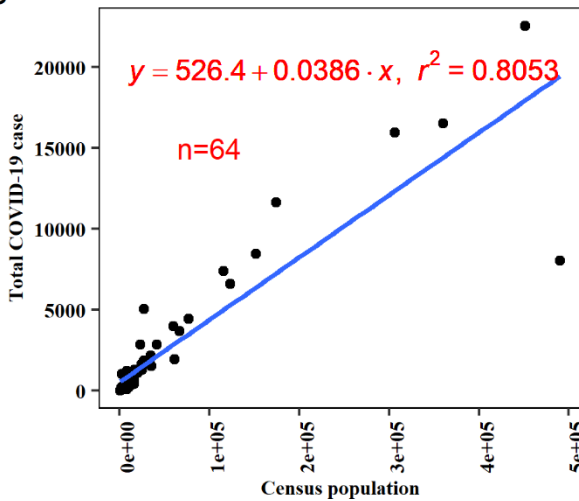
841

842 **Fig. S1.** The relationship between caffeine and paraxanthine concentrations. Plot A included all  
843 the available data, but plot B was without Sikeston Wastewater Treatment Plant (SKSTN).

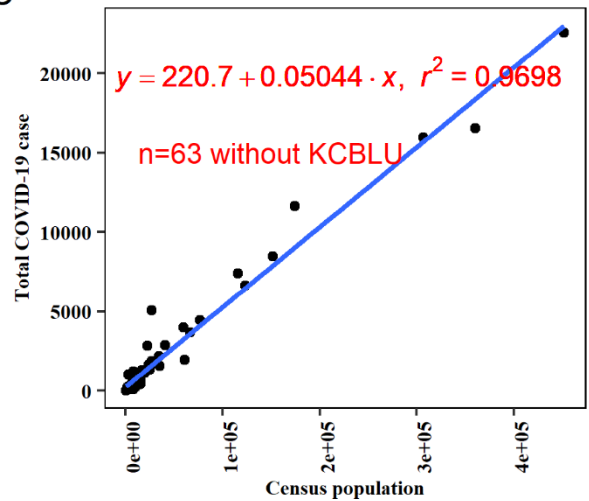
A



B



C



844

845 Fig. S2. A: Predicted real-time populations in the area served by the Kansas City Blue River  
846 wastewater treatment plant (WWTP KCBLU) using concentrations of wastewater biomarkers  
847 based on the models with the data from WWTP KCBLU. The metadata population was plotted  
848 using the orange line for reference. The total Covid-19 clinical cases of each WWTP from  
849 09/13/2021 to 04/10/2022 were strongly increased with the metadata population size (B: with  
850 WWTP KCBLU; C: without WWTP KCBLU).

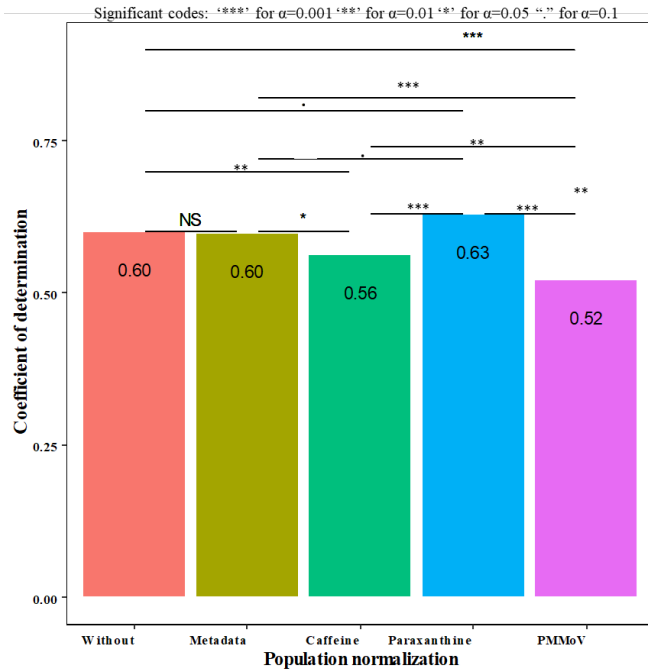
851

852

853

854

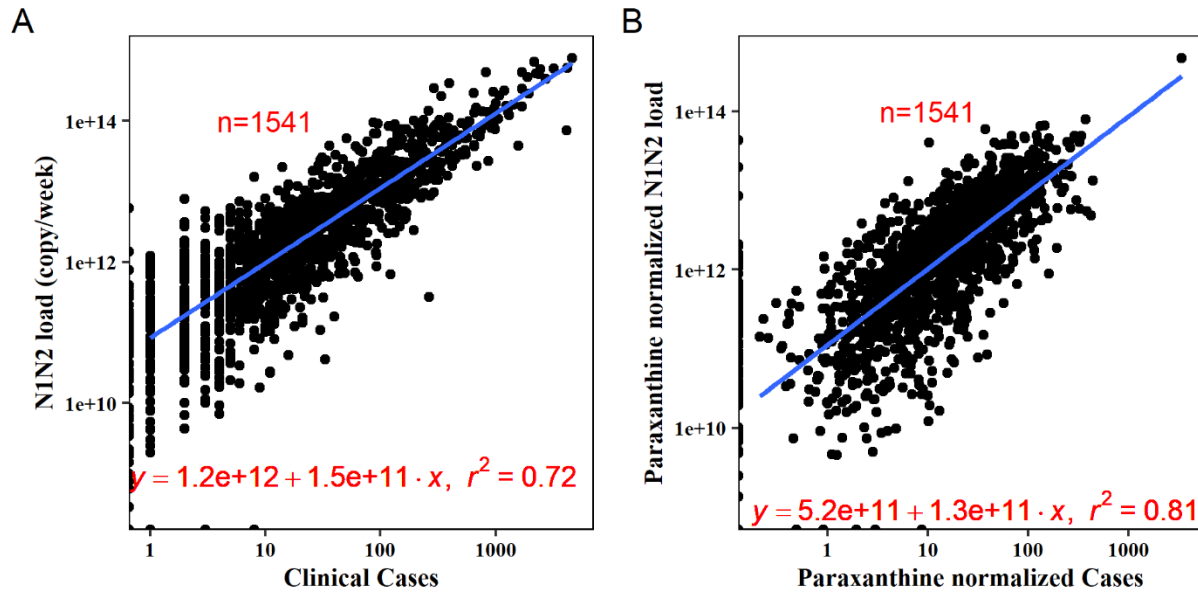
855



856  
857 Fig. S3. Comparison of the coefficient of determination of the linear regression models ( $R^2$ )  
858 between wastewater SARS-CoV-2 RNA load (copies/week/10K person) and clinic COVID-19  
859 incidence rate (cases/week/10K person) within 64 WWTPs without and with the population  
860 normalizations



861



862

863 Fig. S4. The linear regression relationship between wastewater SARS-CoV-2 RNA load with  
864 clinical cases (A: without population normalization; B: paraxanthine population normalization).  
865 The slopes of the regression equation indicated wastewater SARS-CoV-2 RNA concentration per  
866 week and person.

867